2016

# Experimentation with Synthetic Material Disks for Mercury Capture Using an On-Line Mercury Analyzer

Hang Chen
*Lehigh University*

# Experimentation with Synthetic Material Disks for Mercury Capture Using an On-Line Mercury Analyzer

by

Hang Chen

A Thesis

Presented to the Graduate and Research Committee

of Lehigh University

in Candidacy for the Degree of

Master of Science

In

Mechanical Engineering and Mechanics

Lehigh University

May 11, 2016

This thesis is accepted and approved in partial fulfillment of the requirements for the Master of Science.

______________________________

May 11, 2016

______________________________

Dr. Alparslan Oztekin

Thesis Advisor

Department of Mechanical Engineering & Mechanics

Lehigh University

______________________________

Dr. D.Gary Harlow

Department Chairperson

Department of Mechanical Engineering & Mechanics

Lehigh University

# Acknowledgement

I would like to express my sincere gratitude to my thesis advisor Dr. Alparslan Oztekin and Dr. Carlos E. Romero for their valuable guidance and support during my time at the Energy Research Center. I would also like to thank Zheng Yao who is a research scientist at the ERC for his incredible instruction and helping me to complete the experiments. In addition, I am thankful to my fellow graduate students, Zhi Tang and Shaojun Ren for their assistance and discussions regarding the project. Sincere thanks are due to Colleen Munion and Ursla S.Levy who made working at the ERC very enjoyable.

Thank you to all of my family for supporting me during my time at Lehigh University.

# Table of Contents

# List of Tables

# List of Figures

# Abstract

A mercury detection system was built and tested to help assess the mercury absorption ability of synthetic disks, made of Kapton polyimide film, under simulated flue gas conditions at different temperature levels. These synthetic disks would be part of a continuous mercury monitoring system developed by UHV, Inc. and the Lehigh University Energy Research Center. Evaluation of the disks was based on mercury absorption efficiency, calculated from the difference in mercury concentration before and after placing the discs into the detection system. CFD simulations of the temperature field in the test chamber were performed to get an accurate value of the gas temperature at the disk positions. Curve fits for the relationship between mercury absorption efficiency and gas temperature was drawn. This would provide valuable information to be used in the manufacture of the synthetic disk for the UHV mercury analyzer. It was found that the synthetic disks have a better temperature performance in terms of mercury absorption capacity in plain nitrogen flow (60.5% at 150°F) than where the simulated flue gas contains 700 ppm NO, 350 ppm $SO_2$, 12.5% $CO_2$, 5% $O_2$ and $N_2$ balancing the mixture (36.37% at 150 $^oF$). Testing of the disks under simulated flue gas condition with 20% moisture was also performed at 150°F to simulate the conditions of flue gas after a Wet Flue Gas Desulfurization system. The results showed that flue gas humidity has very little impact on the mercury absorption efficiency of the synthetic disks at 150°F.

# 1.0 Introduction

Mercury (Hg) is one of the most volatile heavy metal elements [1]. Hg in the atmosphere can be inhaled by the human body and cause damage to the circulatory system and nervous system, especially to unborn baby's brain. Flue gas released from coal-fired power plants is one of the major sources of Hg pollution.

The Coal-Fired power plants in the U.S. are known to be the main source of the Hg emissions. Mercury Emissions can be in the form of elemental mercury ($Hg^0$) or oxidized mercury（$Hg^{2+}$). The Electrostatic Precipitator (ESP) and Fabric Filters (FF) in these power plants can reduce particulate matter (PM) that includes Hg particulate ($Hg_p$) to a certain extent. Data from actual facilities have indicate that more than 90 % of the $Hg^{2+}$ can be reduced in calcium-based Wet Flue Gas Desulfurization (WFGD) systems. However, it has also been shown that in some situations, $Hg^{2+}$ can be reduced to $Hg^0$ and reemitted with the flue gas, which may lead to a significant decrease of the $Hg$ capturing efficiency of the WFGD [2]. The relatively high volatility, low water solubility and the ability to stay in the atmosphere for half to two years make $Hg^0$ the most uncontrollable form of Hg [3]. Technologies have been developed to control Hg emissions from coal-fired power plants, including dry sorbents, catalysts, scrubbing liquors, flue gas or coal additives, combustion modification, barrier discharges, and ultraviolet radiation for the removal of Hg from flue gas streams [4].

The primary purpose of this study was to test the mercury absorption ability of synthetic disks under different gas streams conditions. These synthetic disks would be part of a continuous $Hg^0$ monitoring system. This system uses Total-reflection X-Ray Fluorescence (TXRF) for $Hg^0$ detection. The Energy Research Center (ERC) is working with UHV, Inc. of KY in this development. During the experiment at the ERC, a mercury generator, simulated flue gas from gas cylinders, a gas heater and a humidifier were used to test the disks under controlled conditions. Using a sealed chamber, a gas stream was flown over the synthetic disks, made of a Kapton Polyimide film, and $Hg^0$ in the simulated flue gas was captured by the disks. The concentration difference of $Hg^0$ between the case of placing the discs in the chamber and not placing the discs in the chamber was used to calculate the $Hg^0$ absorption efficiency of the synthetic discs. $Hg^0$ absorption efficiency of the disks was assessed at different conditions of simulated flue gas concentration, temperature and moisture loading. The FLUENT software was used to simulate the temperature field in the test chamber. This is to assess the realistic value of the gas temperature at the disk positions and get an accurate relationship between the gas temperature and the $Hg^0$ absorption efficiency of the synthetic discs.

# 2.0 Experimental System

The experimental setup is placed in Lab A145 of the ERC. It consists of a CAVKIT mercury generator, stainless steel chamber, a Sir Galahad Analyzer, a gas pump, a heater, gas cylinders, flowmeters and a PFA（Perfluoroalkoxy Alkanes）tubing for connecting the devices (see Figure 1). For the testing of $Hg^0$ concentration with moisture, a humidifier and a dryer were added into the system.

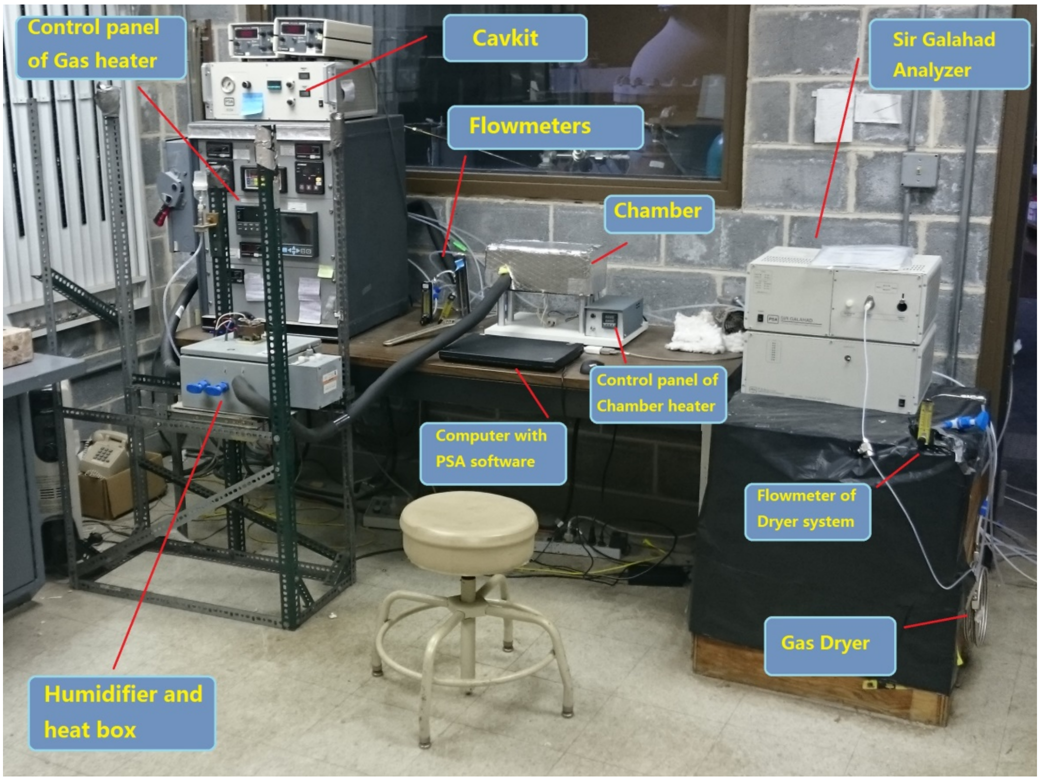


Figure 1: Picture of the System

In the experiment setup, the nitrogen gas from a cylinder carries mercury vapor ( $Hg^0$ ) generated from the CAVKIT reservoir and mixes with simulated flue gas from three gas cylinders. The gas goes through a heater, where it is heated to a stable and controlled temperature, then flows over the sample discs which are placed in an aluminum/ stainless steel chamber as a line shown in Figure 2.

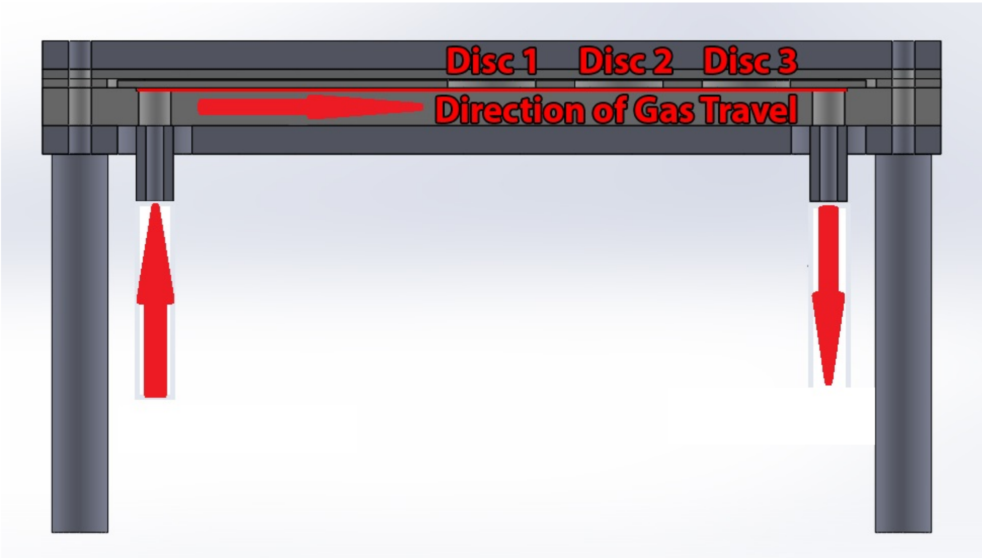


Figure 2: Arrangement of the Disks in the Chamber

Three synthetic discs made of Kapton films were used to capture the $Hg^0$ in the gas stream. These disks would be the choice of material in the future continuous $Hg^0$ analyzer by UHV, Inc. The Sir Galahad analyzer which is a mercury detecting device utilizing Atomic Fluorescence Spectroscopy measures the $Hg^0$ concentration in the gas stream. The system also consists of a gas heater, a pump, gas regulators and cylinders. The gas heater is a stainless steel tube, surrounded by 2 ceramic heating elements. It was used to heat the mixture gas to a controlled temperature so that the inlet temperature of the chamber was high enough and stable for the experimental testing. Figure 3 shows schematic of the system.

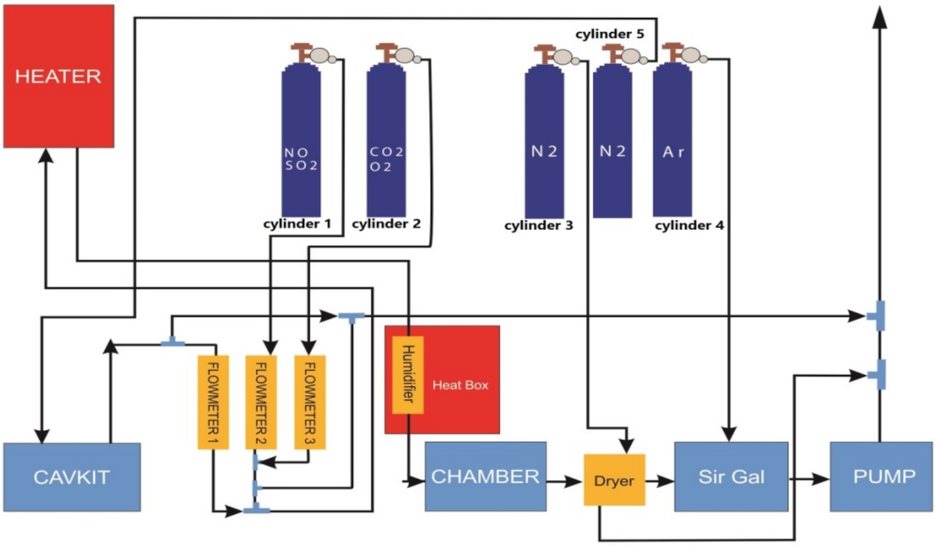


Figure 3: Schematic of the System

## 2.1 Mercury Absorption Capacity Estimating Method

The concentration difference of $Hg^0$ between the case of placing the discs in the chamber and not placing the discs in the chamber was used to calculate the mercury absorption capacity of the synthetic discs. This parameter was important for two reasons:

1) To provide UHV, Inc. with disks doped with $Hg^0$ for analyzer with the TXRF technique for assessment of the detection accuracy of the method.

2) To assess the impact of flue gas conditions on the absorption ability of the disks

Thus, the total flow rate of the simulated flue gas stream, $Q$, is given:

$$Q = Q_{N_2} + Q_{CO_2+O_2+N_2} + Q_{SO_2+NO+N_2} \qquad (1)$$

Where,

$Q_{N_2}$ - Flow rate of the gas stream coming from Cylinder 5 (100 % $N_2$)

$Q_{CO_2+O_2+N_2}$ - Flow rate of the gas stream coming from Cylinder 2 (12.5 % $CO_2$ + 5 % $O_2 + N_2$)

$Q_{SO_2+NO+N_2}$ - Flow rate of the gas stream coming from Cylinder 1 (4 %NO+ 2 % $SO_2 + N_2$)

The Sir Galahad Analyzer was used to detect the mass of $Hg^0$ in the flow. With the known total flow rate of the flue gas stream, $Q$, the $Hg^0$ concentration of the gas stream when the sample discs are in the chamber , $C_1$, and the $Hg^0$ concentration of the gas stream when the sample discs are not in the chamber , $C_2$ ,are calculated as following equation:

$$C_1 = \frac{\sum_1^m M_i}{m \times Q \times t} \qquad (2)$$

$$C_2 = \frac{\sum_1^n M_j}{n \times Q \times t} \qquad (3)$$

$C_1$ - The $Hg^0$ concentration of the gas stream when the sample discs are placed in the chamber

$C_2$ - The $Hg^0$ concentration of the gas stream when the sample discs are not placed in the chamber

$M_j$ - The mass of the $Hg^0$ detected in the gas stream when the sample discs are not in the chamber

$M_i$ - The mass of the $Hg^0$ detected in the gas stream when the sample discs are placed in the chamber

m - The number of times of the test without sample discs in the chamber

n - The number of times of the test with sample discs in the chamber

$t$ - The sampling time for a single test (3 minutes)

In this study, the $Hg^0$ absorption efficiency is used to compare the $Hg^0$ absorption capacity of the synthetic disc at different flow conditions. A higher $Hg^0$ absorption efficiency indicates a better $Hg^0$ absorption capacity of the synthetic disc. The efficiency, $\eta$, can be computed by equation (4):

$$\eta = \frac{C_1 - C_2}{C_1}\% \qquad (4)$$

Equation (5) gives the calculation of the total mass of $Hg^0$ absorbed by one synthetic disk. After testing, the synthetic disks would be sealing packaged and shipped to UHV, Inc. The mass of $Hg^0$ captured by each disc would be tested and compared to this calculation result, $M_{absorb}$ , to determine the credibility of this experiment.

$$M_{absorb} = \frac{1}{3} \times (C_1 - C_2) \times Q \times t' \qquad (5)$$

$t'$ - The time when the three sample discs are in the chamber to absorb elemental mercury

## 2.2 Sample Disk

The discs, made of Kapton film, have a diameter of 2.22 cm as shown in Figure 4. Kapton is a film material, which is synthesized by polymerizing an aromatic diamine and an aromatic dianhydride.

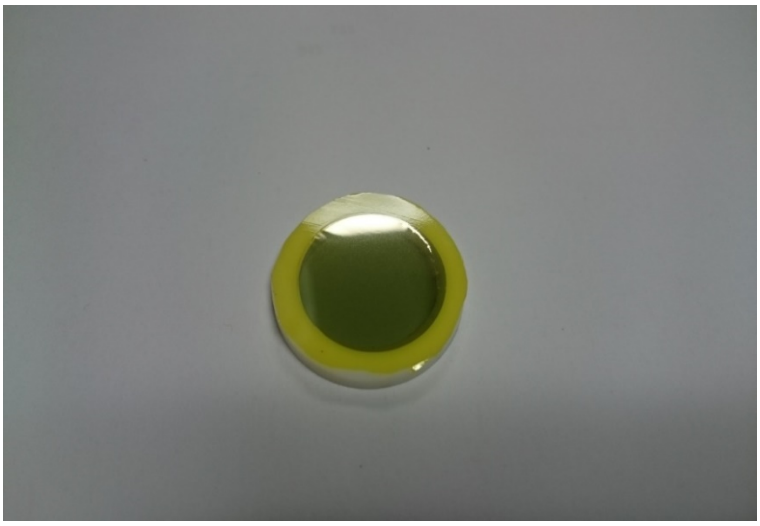

Figure 4: Picture of the Synthetic Disk

The Kapton has many excellent properties of chemical stability, high-temperature resistance, tenacity, abrasive resistance, fire resistance and electric insulativity. Table 1 gives the Chemical Properties of Kapton [5].

Table 1: Chemical Properties of Kapton [5]

| Property | Typical Value: Tensile Retained, % | Typical Value: Elongation Retained, % | Test Condition | Test Method |
|---|---|---|---|---|
| ***Chemical Resistance*** | | | | |
| Isopropyl Alcohol | 96 | 94 | 10 min at 23°C | IPC TM-650 Method 2.2.3B |
| Toluene | 99 | 91 | | |
| Methyl Ethyl Ketone | 99 | 90 | | |
| Methylene Chloride/ Trichloroethylene (1:1) | 98 | 85 | | |
| 2 N Hydrochloric Acid | 98 | 89 | | |
| 2 N Sodium Hydroxide | 82 | 54 | | |
| ***Fungus Resistance*** | Nonnutrient | | | IPC TM-650 Method 2.6.1 |
| ***Moisture Absorption*** | 1.8% Types HN and VN | | 50% RH at 23°C | ASTM D-570-81 (1988)$^{\epsilon 1}$ |
| | 2.8% Types HN and VN | | Immersion for 24 h at 23°C (73°F) | |
| ***Hygroscopic Coefficient of Expansion*** | 22 ppm/% RH | | 23°C (73°F), 20–80% RH | |
| ***Permeability*** | | | | |
| ***Gas*** | *mL/m$^2$·24 h·MPa* | *cc/(100 in$^2$·24 h·atm)* | 23°C (73°F), 50% RH | ASTM D-1434-82 (1988)$^{\epsilon 1}$ |
| Carbon Dioxide | 6840 | 45 | | |
| Oxygen | 3800 | 25 | | |
| Hydrogen | 38,000 | 250 | | |
| Nitrogen | 910 | 6 | | |
| Helium | 63,080 | 415 | | |
| ***Vapor*** | *g/(m$^2$·24 h)* | *g/(100 in$^2$·24 h)* | | ASTM E-96-92 |
| Water | 54 | 3.5 | | |

## 2.3 Devices

The experimental devices include a CAVKIT mercury generator, Sir Galahad analyzer, an aluminum/ stainless steel chamber, a humidifier with a heating box, a dryer, a gas heater and a pump. PFA tubing was used to connect the devices.

## 2.3.1 PSA calibration gas generator (CAVKIT):

The CAVKIT is a device comprised of a mercury reservoir, flow meters and a pressure regulator all connected by Teflon tubing, as shown in Figure 5.

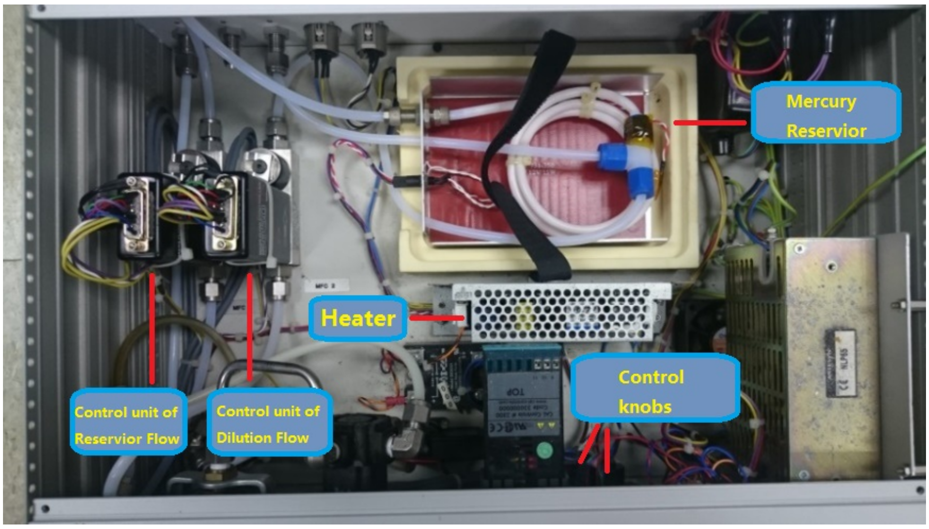


Figure 5: Photo of the Inside Structure of CAVKIT

Nitrogen gas comes from a gas cylinder, at a controlled low flow rate, is passed over the CAVKIT mercury reservoir to carry a calibrated amount of mercury vapor and mix with another $N_2$ flow, which is acted as the dilution flow. The reservoir is set to a steady temperature so that the mercury generated from the reservoir has a known amount which can be adjusted with temperature. The higher the temperature is, the more the $Hg^0$ vapor is generated, leading to a higher mercury concentration in the reservoir flow and the final gas stream. The schematic diagram of CAVKIT is shown in Figure 6 [7].

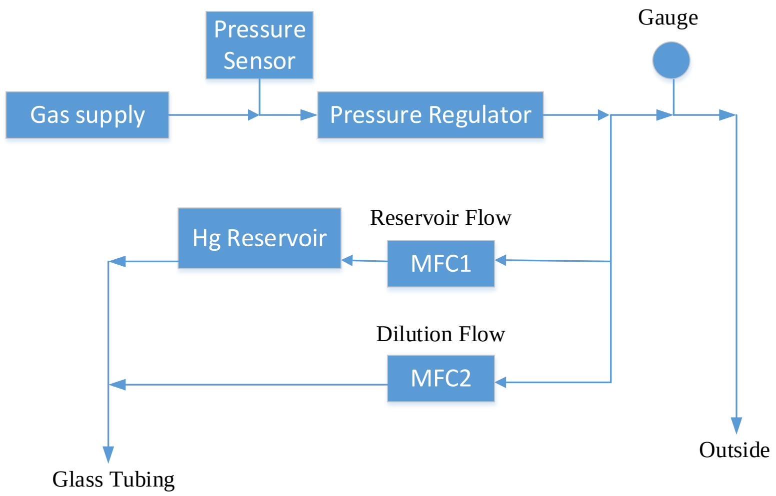


Figure 6: Schematic Diagram of CAVKIT

### 2.3.2 Sir Galahad Analyzer:

The Sir Galahad 2 analyzer is an analytical instrument produced by P S Analytical (PSA), which can be used to semi-continuously monitor and measure the concentration of $Hg^0$ in gaseous samples. A gold trap is placed in the instrument which can amalgamate with $Hg^0$ carried by an input gas flow after being heated to a low temperature level (100℃-150℃) [4]. After being continuously heated to 800℃ under controlled conditions, the $Hg^0$ is released separately which can be detected and measured by a fluorescent detector, using atomic fluorescence spectrometry. The PSA software calculates the mass of $Hg^0$ based on the amount of photons released. After the heating process, the gold trap is flushed with Argon, which helps cleaning the trap and carries the residual $Hg^0$ away from the trap.

## 2.3.3 Chamber

Two test chambers were used in the experiment. They have the same size of 12" x 4" x 1.5" [6], one was made of aluminum and the other was stainless steel. Figure 8 shows the structure of the chambers.

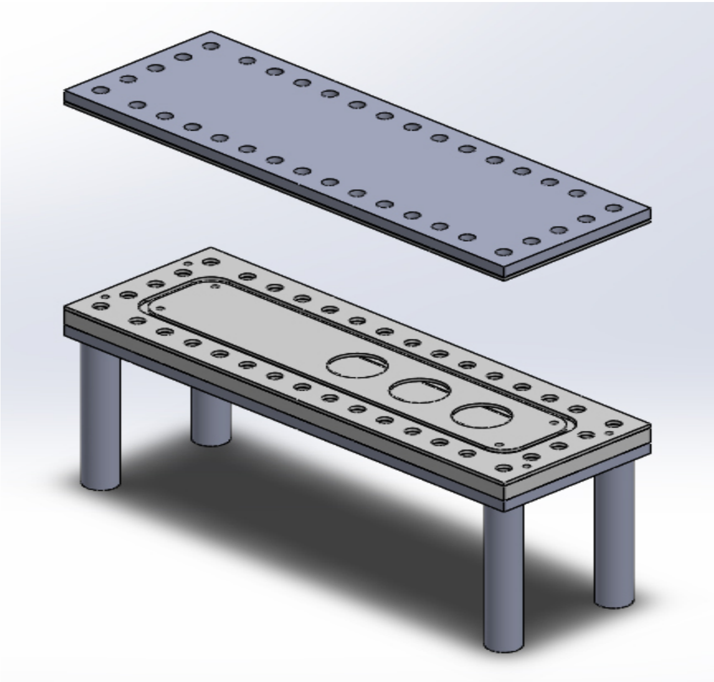

Figure 7: The Chamber Structure

An O-ring of 4 mm in diameter is placed around the discs to seal the disk's chamber. The internal channel has dimensions of 0.036" x 0.9" x 8.5". The three sample discs are placed inside the chamber to allow the simulated gas stream to flow over the Kapton disks and allow $Hg^0$ to be captured.

In the first group of tests at ambient temperature ($68\,^oF$) in 100% nitrogen flow, only the aluminum chamber was used. In further tests at $100\,^oF$, $150\,^oF$ and 200

$^{o}F$ with nitrogen flow or mixture of the gases, the stainless steel chamber was used instead of the aluminum chamber to avoid deformation of the chamber.

## 2.3.4 Humidifier and Dryer

In $Hg^{0}$ absorption tests with moisture, a humidifier was placed upstream of the inlet of the chamber, to generate steam and simulate a wet stack condition of the flue gas. A dryer was used to remove steam in the gas stream between the chamber and the Sir Galahad analyzer so that the analyzer would provide an accurate result. Moisture impairs the gold amalgamation process for $Hg^{0}$ and plugs the gold trap.

### 2.3.4.1 Humidifier

The tube-in-shell humidifier, MH-110-12F from Perma Pure LLC, was used as shown in Figure 8. A pressure difference between the water and inlet gas flow makes the water vapor permeate through the internal tube and evaporate into the gas stream. During the $Hg^{0}$ absorption test in simulated gas flow at 150 $^{o}F$ with increased moisture level, the outer shell of the humidifier was heated by a heater box to a controlled temperature, which equals or above the temperature at which the air will be saturated (dew point).

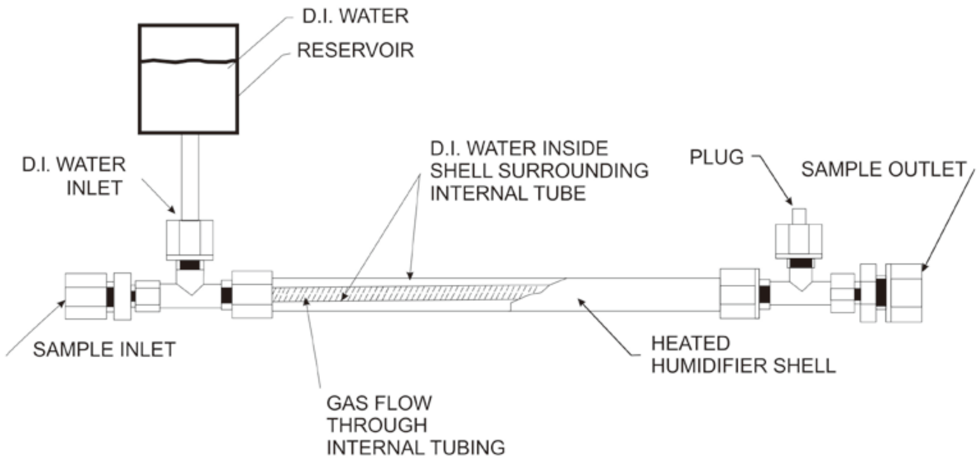


Figure 8: Schematic Drawing of the Humidifier

### 2.3.4.2 Dryer

The dryer, MD-110-144S from Perma Pure LLC, is a shell and tube moisture exchanger as shown in Figure 9. In this device, simulated flue gas and purge gas are placed as two countercurrent flow streams on the two sides of the internal tube. The water concentration differential between the purge gas and the moist sample gas stream drives the water to permeate through an internal Nafion Tube and evaporate into the purge gas stream so that the samples gas is dried.

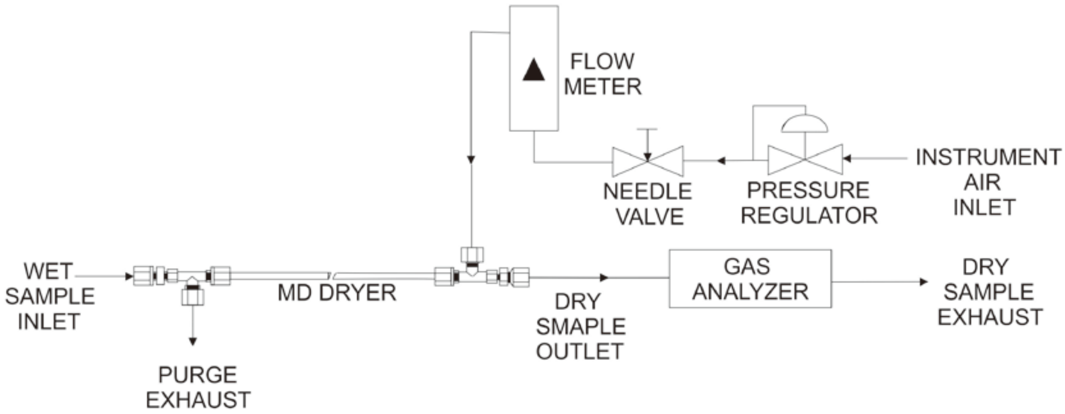


Figure 9: Schematic Drawing of the Dryer

### 2.3.4.3 Humidity Estimation:

To simulate the humidity condition of the stack flue gas after WFGD, the humidity in the gas stream should be set at around 20%. The water vapor generating ability of the humidifier was examined under the experimental flow condition.

The glass container, as figure 10 shows, was used as the water reservoir in the humidifier system.

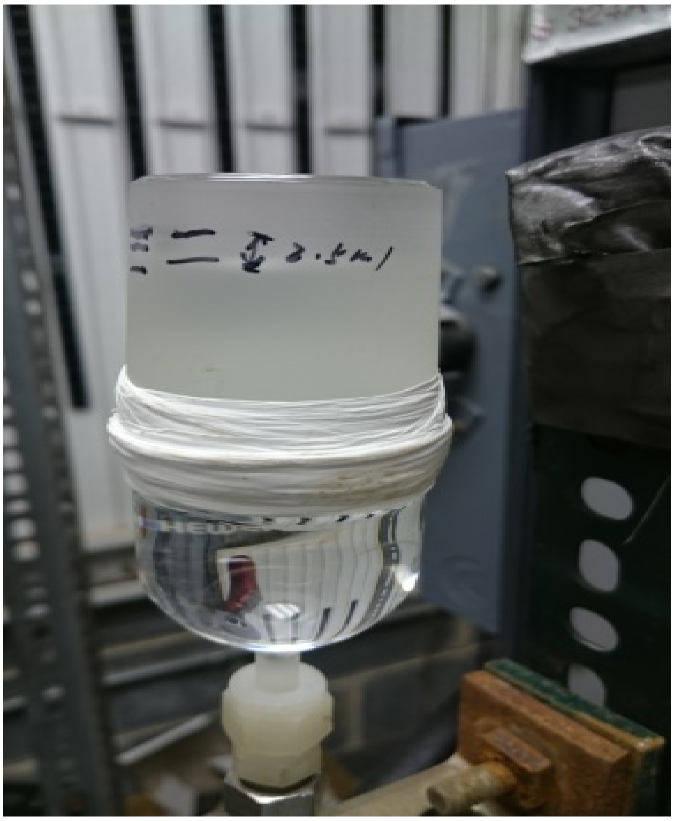

Figure 10: The Glass Container

To estimate the moisture generated into the gas stream, a certain volume of water was injected into the glass container, a scale was drawn to show the water level of the container. 2.5 ml of water was injected by the syringe into the container, which led to a new water level. Another scale was drawn to show the new water level, so that the volume of water between two scales was 2.5ml. After that, experimental devices were turned on to simulate the testing condition, the humidifier started to generate water vapor into the gas stream. The time of consuming 2.5ml of water was recorded. With the known flow rate and components of the gas stream, the humidity of the gas stream was calculated.

# 3.0 Experimentation and Simulations

Aiming at determining $Hg^0$ absorption capacity for the synthetic discs under simulated flue gas conditions, experiments were first conducted using only nitrogen as the carrier gas (Case-1), followed by a mixture of gas, representing a typical flue gas composition from a coal-fired unit (Case-2), finalizing with experiments using a simulated flue gas with increased moisture level representing a coal-fired unit wet stack (Case-3). There were four temperature levels of the inlet gas stream: ambient temperature, $100\,^oF$ , $150\,^oF$ and $200\,^oF$ used in the experiment. However, in the early experiments in 100% nitrogen flow, the edge of the synthetic discs were burned at 200°F by the heater inside the stainless steel chamber, so in the follow-on experiments, gas was not heated to the $200\,^oF$ level. For the tests with the simulated stack flue gas, the gas components were set at 700 ppm NO, 350 ppm $SO_2$, 12.5% $CO_2$, 5% $O_2$ and $N_2$ balancing the mixture. For the tests in simulated stack flue gas with increased moisture level, the gas components were set at 700 ppm NO, 350 ppm $SO_2$, 12.5% $CO_2$, 5% $O_2$, $N_2$ balancing the mixture with a moisture level humidity around 20%. Table 2 shows the matrix of experimental conditions.

Table 2: Experimental Conditions

| Case Number | $Hg^0$ Concentration of the Gas Stream | Gas Components | Inlet Gas Temperature | Total Flow Rate | |
|---|---|---|---|---|---|
| Case-1 | 5 ng/L | $N_2$ only | Ambient Temperature (68$^oF$) | Round-1 | 0.44 L/min |
| | | | 100$^oF$ | | 0.4 L/min |
| | | | 150$^oF$ | | 0.4 L/min |
| | | | 200$^oF$ | | 0.2 L/min |
| | | | Ambient Temperature (59$^oF$) | Round-2 | 0.4 L/min |
| | | | 100$^oF$ | | 0.4 L/min |
| | | | 150$^oF$ | | 0.4 L/min |
| | | | 200$^oF$ | | 0.4 L/min |
| Case-2 | 5 ng/L | Mixture Gas (700 ppm NO, 350 ppm $SO_2$, 12.5% $CO_2$, 5% $O_2$, $N_2$ acting as the balance gas) | Ambient Temperature (59$^oF$) | 0.4 L/min | |
| | | | 100$^oF$ | 0.51 L/min | |
| | | | 150$^oF$ | 0.4 L/min | |
| Case-3 | 5 ng/L | Mixture Gas with Moisture (700 ppm NO, 350 ppm $SO_2$, 12.5% $CO_2$, 5% $O_2$, $N_2$ acting as the balance gas) 20% $H_2O$ | 150$^oF$ | 0.3 L/min | |

The CAVKIT was used as a $Hg^0$ vapor generator and during the testing, the concentration of the $Hg^0$ in the gas stream was controlled at a stable level to simulate the $Hg^0$ emissions condition in a typical coal-fired unit flue gas. The method to control the $Hg^0$ concentration in the test stream was to adjust the CAVKIT reservoir flow rate, based on the $Hg^0$ concentration detected by Sir Galahad Analyzer. To make sure that the measurements with the Sir Galahad Analyzer were accurate, an analyzer calibration was needed [7].

The calibration procedure involves the injection of $Hg^0$ vapor at a set temperature onto the gold trap. This is a simple but effective means of providing a primary standard which is more effective than the alternative diffusion tube approached and is also considerably more economic [10]. Standard $Hg^0$ vapor was introduced into an argon stream via a septum. This allowed a syringe to be inserted directly into the argon flow path and thus directly over the gold trap. The $Hg^0$ used as a primary standard was contained in a specially designed glass container maintained at atmosphere pressure which was held in a thermostatic bath. The temperature of the $Hg^0$ in the container was monitored using a thermometer, as shown in Figure 11.

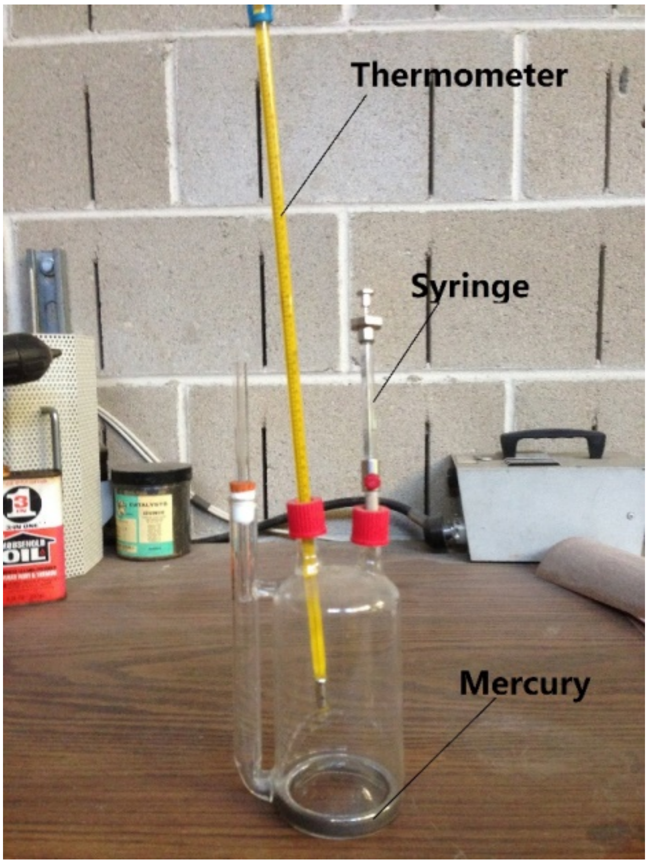


Figure 11: $Hg^0$ Vapor Container, Thermometer and Syringe

Several volumes of saturated $Hg^0$ vapor were injected by the syringe into the calibration port of the Sir Galahad Analyzer. The PSA software produced the signal peak height recorded by the Atomic fluorescence Spectrometry detector in the Sir Galahad. A curve of mass of $Hg^0$ vs. peak height was then obtained. In this study, this curve was used to calculate the $Hg^0$ mass in the gas stream using a detected signal peak height. The calibration data and curve are shown in Table 3 and Figure 12.

Table 3: Sir Galahad Analyzer Calibration Data

| | Temperature | Volume | Mass | Peak Height | Date | Time |
|---|---|---|---|---|---|---|
| Unit | °C | ml | ng | | | |
| 1 | 10.50 | 0.00 | 0.00000 | 33.41000 | 07/03/16 | 13:34:37 |
| 2 | 11.20 | 3000.00 | 18.52000 | 1109.63000 | 07/03/16 | 13:37:56 |
| 3 | 11.20 | 1000.00 | 6.17333 | 403.14999 | 07/03/16 | 13:41:14 |
| 4 | 11.20 | 2000.00 | 12.34667 | 818.51001 | 07/03/16 | 13:44:38 |
| 5 | 11.20 | 600.00 | 3.70400 | 246.75999 | 07/03/16 | 13:47:48 |
| 6 | 11.20 | 300.00 | 1.85200 | 134.21001 | 07/03/16 | 13:51:08 |
| 7 | 11.20 | 50.00 | 0.30867 | 43.77000 | 07/03/16 | 13:54:20 |

**Unit : ng**

**Slope : 59.84424**

**Y Intercept : 31.69178**

**Correlation Coefficient : 0.99836**

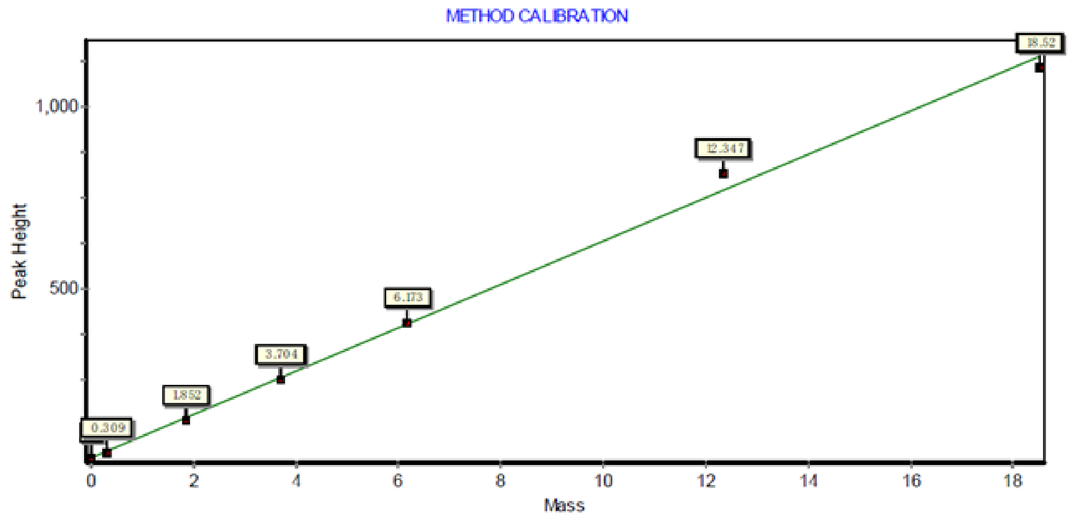


Figure 12: Sir Galahad Analyzer Calibration Curve

For the experimental process, the gas heater, the CAVKIT mercury generator, gas pump and the Sir Galahad Analyzer were turned on firstly, and the valves on the regulators of the cylinders were opened to let the gas flow into the system. After the display on the gas heater control panel reached the target temperature, flowmeters were used to control the flow rates of different gas sources to meet the experimental condition for each particular run. The trap cleaning function of the PSA analyzer was used for each run to make the Sir Galahad Analyzer clean the trap with hydrogen to avoid residual $Hg^{\circ}$, which would lead to a biased $Hg^{\circ}$ level in the gas stream. The PSA analyzer was run continuously to monitor the $Hg^{\circ}$ concentration in the gas stream. After several rounds of testing (every round last for 5 minutes and 45 seconds), when the concentration of $Hg^{\circ}$ detected become to be stable, the most recent 3-4 rounds of test data of the $Hg^{\circ}$ concentration were recorded. After that, the test chamber was opened and three synthetic discs were placed on the preset positions inside the chamber, then the chamber was closed. The Sir Galahad Analyzer continuously monitored the $Hg^{\circ}$ concentration in the gas stream. The data of the first two rounds of testing after putting discs into the chamber was recorded. Finally, the chamber was opened and three disks were removed and sealing packaged separately.

The temperature measured in the test was the inlet gas stream temperature, which was close to but does not completely equal to the temperature at the position of the synthetic discs. The heat loss along the chamber internal channel led to a temperature difference between the inlet gas stream temperature and the temperature at the disk positions, as shown in Figure 13. The $Hg^0$ absorption efficiency of the synthetic disks would be significantly impacted by the gas stream temperature, so a little temperature difference could lead to a huge error of the relationship between the $Hg^0$ absorption efficiency and the gas stream temperature at the disk position. Therefore, a realistic temperature value of the gas stream flowing right over the disc positions was needed.

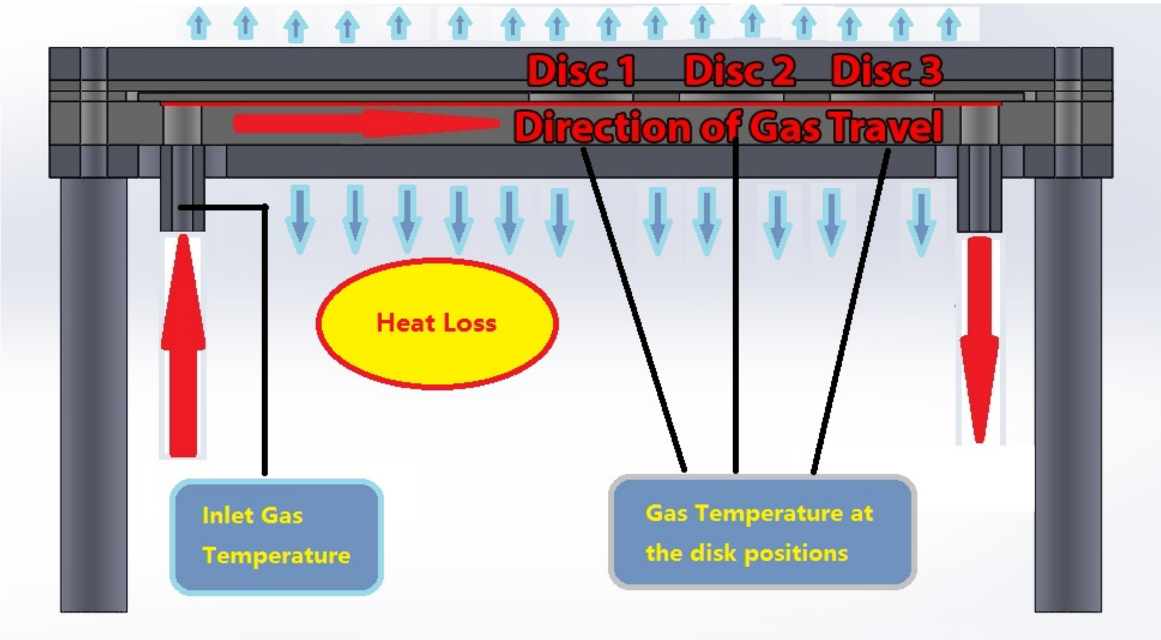


Figure 13: Heat Loss of the Gas Stream inside the Chamber

A CFD (Computational Fluid Dynamics) simulation was performed to get the accurate temperature of the gas stream flowing right over the disc position. A 3-D model of the internal structure of the chamber was built, as Figure 14 shown. The temperature field inside the chamber was modeled by using the software FLUENT. The intension was to get a realistic value of the gas temperature at the disc positions.

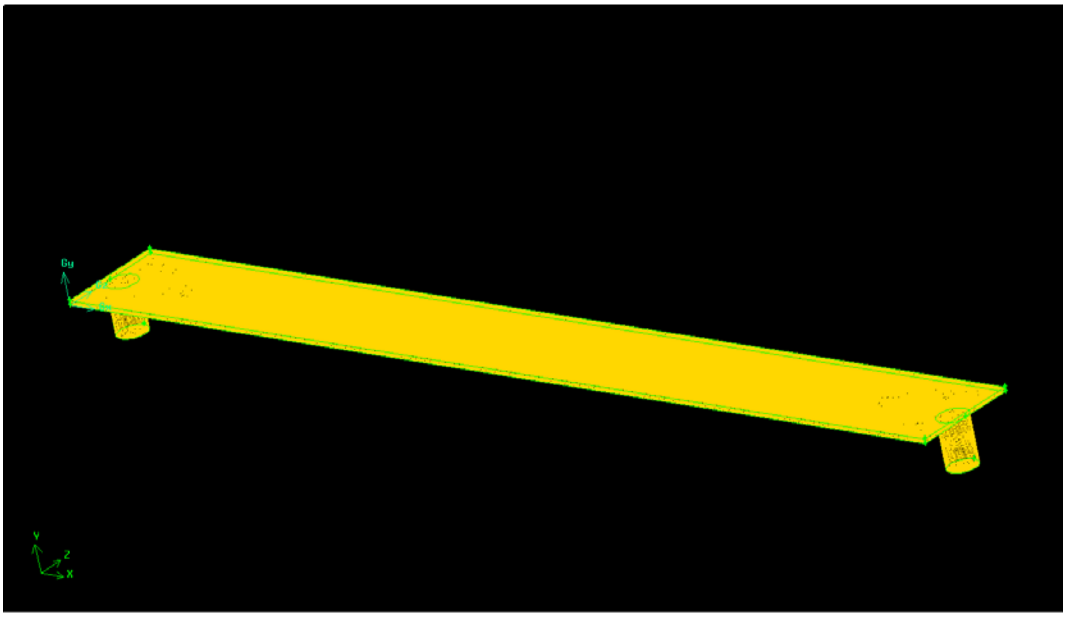

Figure 14: 3-D Gambit Model of the Chamber

The mesh was checked and quality was obtained. The solver was changed to Pressure-Based type. The velocity formulation was changed to absolute and time to steady state. Energy was set to ON position. Laminar viscous flow was used as the viscous model. The material used as wall material was stainless steel from the FLUENT database and the flow was assumed to be nitrogen in Case-1 and stack gas in Case-2. For cell zone conditions, the parts were assigned as nitrogen/ stack gas as fluid parts and stainless steel as solid parts. Boundary conditions were applied according to the need of the model. The inlet condition was defined as velocity inlet and outlet was set as pressure outlet. The inlet gas velocity was calculated based on the known total flow rate and inlet cross section area. The inlet gas temperature was measured by a thermocouple. The wall temperature, which was the temperature of the chamber internal surface, was detected by a thermocouple placed inside the chamber. The convective heat coefficient of the wall was assumed to be $1 W/m^2 * K$ [8]. Solution methods were specified as following:

- Scheme =Simple
- Gradient= Least square cell based
- Pressure= Second order
- Momentum= Second order upwind
- Energy= Second order upwind

Then the initialization method was set to Standard Initialization. The hot inlet was selected from the drop down list and the solution was initialized.

# 4.0 Results

## 4.1 Case-1: Nitrogen Flow

Two rounds of testing (Round-1 and Round-2) were performed under a condition of 100% nitrogen flow and in each round, there were four groups of tests run at four different temperature levels (ambient temperature, 100 $^{o}F$ , 150 $^{o}F$ and 200 $^{o}F$ ) to shake down the experimental system, and obtain baseline data on the performance of the synthetic disks, in terms of this Hg° absorption capacity. The Hg° concentration was set at 5 ng/ L to simulate a low mercury emissions level in the stack flue gas.

The first four groups of testing (Round-1) produced Hg° absorption results that were erratic with respect to the inlet gas temperatur. It was found that the edge of the disk was burnt by the heat from the heater inside the chamber, which randomly affected the Hg° absorption ability of the synthetic disks. Therefore, another four groups of tests (Round-2) were performed, in which the heater in the chamber was not turned on during testing. For these Round-2 tests, the gas heater was set at a higher temperature than in Round-1, to offset the influence of not using the heater in the chamber.

### 4.1.1 Test Results

Table 4： Test Result for 100% $N_2$ Gas Experiment (Round 1, Ambient Temperature, 68°F)

| Round-1-1 | | | | | | | | | | | | | | | |
|---|---|---|---|---|---|---|---|---|---|---|---|---|---|---|---|
| Date | Sample Discs in the Chamber | Total Flow | Flowmeter 1 | Flowmeter 2 | Flowmeter 3 | Simulated Flue Gas Components | | | | | Flow Sampling Time | Total Sampling Volume | PSA Measurement Value | Hg Concentration in Sample Gas | Absorption |
| | | | N2+Hg | SO2 (4%) + NO (2%) + N2 (balance) | CO2 (25%) + O2 (10%) + N2(balance) | SO2 | NO | CO2 | O2 | N2 | | | | | |
| | | L/min | L/min | L/min | L/min | ppm | ppm | % | % | % | min | L | ng | ng/L | ng |
| 2015/10/13 | No Sample | 0.44 | 0.44 | 0 | 0 | 0 | 0 | 0.00% | 0.00% | 0.00% | 3 | 1.32 | 7.81 | 5.92 | |
| 2015/10/13 | No Sample | 0.44 | 0.44 | 0 | 0 | 0 | 0 | 0.00% | 0.00% | 0.00% | 3 | 1.32 | 7.76 | 5.88 | |
| 2015/10/13 | No Sample | 0.44 | 0.44 | 0 | 0 | 0 | 0 | 0.00% | 0.00% | 0.00% | 3 | 1.32 | 7.77 | 5.89 | |
| 2015/10/13 | No Sample | 0.44 | 0.44 | 0 | 0 | 0 | 0 | 0.00% | 0.00% | 0.00% | 3 | 1.32 | 7.78 | 5.90 | |
| 2015/10/13 | 3 Discs | 0.44 | 0.44 | 0 | 0 | 0 | 0 | 0.00% | 0.00% | 0.00% | 3 | 1.32 | 4.41 | 3.34 | 3.37 |
| 2015/10/13 | 3 Discs | 0.44 | 0.44 | 0 | 0 | 0 | 0 | 0.00% | 0.00% | 0.00% | 3 | 1.32 | 4.24 | 3.21 | 3.54 |

Table 4 shows test data of Round-1 under inlet gas stream conditions of nitrogen flow only, at ambient temperature (68 $^oF$ ). When the disks were not placed in the chamber, the detected $Hg^0$ concentrations at the outlet of the chamber were 5.92 ng/L, 5.88 ng/L, 5.89 ng/L and 5.90 ng/L. After the synthetic disks were put into the chamber, $Hg^0$ concentrations were detected as: 3.34ng/L and 3.21 ng/L. The $Hg^0$ capturing capacity of the disks led to the difference of $Hg^0$ concentration in the gas stream.

Table 5: Test Result for 100% $N_2$ Gas Experiment (Round 1,100 $^{o}F$ )

| Round-1-2 | | | | | | | | | | | | | | | |
|---|---|---|---|---|---|---|---|---|---|---|---|---|---|---|---|
| Date | Sample Discs in the Chamber | Total Flow | Flowmeter 1 | Flowmeter 2 | Flowmeter 3 | Simulated Flue Gas Components | | | | | Flow Sampling Time | Total Sampling Volume | PSA Measurement Value | Hg Concentration in Sample Gas | Absorption |
| | | | N2+Hg | SO2 (4%) + NO (2%) + N2 (balance) | CO2 (25%) + O2 (10%) + N2 (balance) | SO2 | NO | CO2 | O2 | N2 | | | | | |
| | | L/min | L/min | L/min | L/min | ppm | ppm | % | % | % | min | L | ng | ng/L | ng |
| 2015/10/20 | No Sample | 0.4 | 0.4 | 0 | 0 | 0 | 0 | 0.00% | 0.00% | 0.00% | 3 | 1.2 | 7.50 | 6.25 | |
| 2015/10/20 | No Sample | 0.4 | 0.4 | 0 | 0 | 0 | 0 | 0.00% | 0.00% | 0.00% | 3 | 1.2 | 7.92 | 6.60 | |
| 2015/10/20 | No Sample | 0.4 | 0.4 | 0 | 0 | 0 | 0 | 0.00% | 0.00% | 0.00% | 3 | 1.2 | 7.11 | 5.93 | |
| 2015/10/20 | No Sample | 0.4 | 0.4 | 0 | 0 | 0 | 0 | 0.00% | 0.00% | 0.00% | 3 | 1.2 | 6.90 | 5.75 | |
| 2015/10/20 | 3 Discs | 0.4 | 0.4 | 0 | 0 | 0 | 0 | 0.00% | 0.00% | 0.00% | 3 | 1.2 | 0.00 | 0.00 | 7.36 |
| 2015/10/20 | 3 Discs | 0.4 | 0.4 | 0 | 0 | 0 | 0 | 0.00% | 0.00% | 0.00% | 3 | 1.2 | 1.27 | 1.06 | 6.09 |

Table 5 shows test data of Round-1 under inlet gas stream conditions of nitrogen flow only, at 100°F. When the disks were not placed in the chamber, the detected $Hg^0$ concentrations at the outlet of the chamber were 6.25 ng/L, 6.60 ng/L, 5.93 ng/L and 5.75 ng/L. After the synthetic disks were put into the chamber, $Hg^0$ concentrations were detected as: 0.00 ng/L and 1.06 ng/L. The $Hg^0$ capturing capacity of the disks led to the difference of $Hg^0$ concentration in the gas stream.

Table 6: Test Result for 100% $N_2$ Gas Experiment (Round 1,150 $^oF$ )

| Round-1-3 | | | | | | | | | | | | | | | |
|---|---|---|---|---|---|---|---|---|---|---|---|---|---|---|---|
| Date | Sample Discs in the Chamber | Total Flow | Flowmeter 1 | Flowmeter 2 | Flowmeter 3 | Simulated Flue Gas Components | | | | | Flow Sampling Time | Total Sampling Volume | PSA Measurement Value | Hg Concentration in Sample Gas | Absorption |
| | | | N2+Hg | SO2 (4%) + NO (2%) + N2 (balance) | CO2 (25%) + O2 (10%) + N2 (balance) | SO2 | NO | CO2 | O2 | N2 | | | | | |
| | | L/min | L/min | L/min | L/min | ppm | ppm | % | % | % | min | L | ng | ng/L | ng |
| 2015/10/21 | No Sample | 0.4 | 0.4 | 0 | 0 | 0 | 0 | 0.00% | 0.00% | 0.00% | 3 | 1.2 | 13.20 | 11.00 | |
| 2015/10/21 | No Sample | 0.4 | 0.4 | 0 | 0 | 0 | 0 | 0.00% | 0.00% | 0.00% | 3 | 1.2 | 10.08 | 8.40 | |
| 2015/10/21 | No Sample | 0.4 | 0.4 | 0 | 0 | 0 | 0 | 0.00% | 0.00% | 0.00% | 3 | 1.2 | 11.44 | 9.54 | |
| 2015/10/21 | 3 Discs | 0.4 | 0.4 | 0 | 0 | 0 | 0 | 0.00% | 0.00% | 0.00% | 3 | 1.2 | 6.36 | 5.30 | 5.22 |
| 2015/10/21 | 3 Discs | 0.4 | 0.4 | 0 | 0 | 0 | 0 | 0.00% | 0.00% | 0.00% | 3 | 1.2 | 5.43 | 4.53 | 6.14 |

Table 6 shows test data of Round-1 under inlet gas stream conditions of nitrogen flow only, at 150°F. When the disks were not placed in the chamber, the detected $Hg^0$ concentrations at the outlet of the chamber were 11.00 ng/L, 8.40 ng/L and 9.54 ng/L. After the synthetic disks were put into the chamber, $Hg^0$ concentrations were detected as: 5.30ng/L and 4.53 ng/L. The $Hg^0$ capturing capacity of the disks led to the difference of $Hg^0$ concentration in the gas stream.

Table 7: Test Result for 100% $N_2$ Gas Experiment (Round 1,200 $^{o}F$ )

| Round-1-4 | | | | | | | | | | | | | | | |
|---|---|---|---|---|---|---|---|---|---|---|---|---|---|---|---|
| Date | Sample Discs in the Chamber | Total Flow | Flowmeter 1 | Flowmeter 2 | Flowmeter 3 | Simulated Flue Gas Components | | | | | Flow Sampling Time | Total Sampling Volume | PSA Measurement Value | Hg Concentration in Sample Gas | Absorption |
| | | | N2+Hg | SO2 (4%) + NO (2%) + N2 (balance) | CO2 (25%) + O2 (10%) + N2 (balance) | SO2 | NO | CO2 | O2 | N2 | | | | | |
| | | L/min | L/min | L/min | L/min | ppm | ppm | % | % | % | min | L | ng | ng/L | ng |
| 2015/10/26 | No Sample | 0.2 | 0.2 | 0 | 0 | 0 | 0 | 0.00% | 0.00% | 0.00% | 3 | 0.6 | 19.94 | 33.24 | |
| 2015/10/26 | No Sample | 0.2 | 0.2 | 0 | 0 | 0 | 0 | 0.00% | 0.00% | 0.00% | 3 | 0.6 | 19.18 | 31.97 | |
| 2015/10/26 | No Sample | 0.2 | 0.2 | 0 | 0 | 0 | 0 | 0.00% | 0.00% | 0.00% | 3 | 0.6 | 21.72 | 36.20 | |
| 2015/10/26 | No Sample | 0.2 | 0.2 | 0 | 0 | 0 | 0 | 0.00% | 0.00% | 0.00% | 3 | 0.6 | 21.86 | 36.44 | |
| 2015/10/26 | 3 Discs | 0.2 | 0.2 | 0 | 0 | 0 | 0 | 0.00% | 0.00% | 0.00% | 3 | 0.6 | 3.46 | 5.77 | 17.21 |
| 2015/10/26 | 3 Discs | 0.2 | 0.2 | 0 | 0 | 0 | 0 | 0.00% | 0.00% | 0.00% | 3 | 0.6 | 0.00 | 0.00 | 20.68 |

Table 7 shows test data of Round-1 under inlet gas stream conditions of nitrogen flow only, at 200°F. When the disks were not placed in the chamber, the detected $Hg^0$ concentrations at the outlet of the chamber were 33.24 ng/L, 31.97 ng/L, 36.20 ng/L and 36.44 ng/L. After the synthetic disks were put into the chamber, $Hg^0$ concentrations were detected as: 5.57ng/L and 0.00 ng/L. The $Hg^0$ capturing capacity of the disks led to the difference of $Hg^0$ concentration in the gas stream.

Table 8: Test Result for 100% $N_2$ Gas Experiment (Round 2, Ambient Temperature, 59°F)

| Round-2-1 | | | | | | | | | | | | | | | |
|---|---|---|---|---|---|---|---|---|---|---|---|---|---|---|---|
| Date | Sample Discs in the Chamber | Total Flow | Flowmeter 1 | Flowmeter 2 | Flowmeter 3 | Simulated Flue Gas Components | | | | | Flow Sampling Time | Total Sampling Volume | PSA Measurement Value | Hg Concentration in Sample Gas | Absorption |
| | | | N2+Hg | SO2 (4%) + NO (2%) + N2 (balance) | CO2 (25%) + O2 (10%) + N2 (balance) | SO2 | NO | CO2 | O2 | N2 | | | | | |
| | | L/min | L/min | L/min | L/min | ppm | ppm | % | % | % | min | L | ng | ng/L | ng |
| 2015/11/10 | No Sample | 0.4 | 0.4 | 0 | 0 | 0 | 0 | 0.00 % | 0.00 % | 0.00 % | 3 | 1.2 | 7.07 | 5.89 | |
| 2015/11/10 | No Sample | 0.4 | 0.4 | 0 | 0 | 0 | 0 | 0.00 % | 0.00 % | 0.00 % | 3 | 1.2 | 6.74 | 5.61 | |
| 2015/11/10 | No Sample | 0.4 | 0.4 | 0 | 0 | 0 | 0 | 0.00 % | 0.00 % | 0.00 % | 3 | 1.2 | 6.93 | 5.77 | |
| 2015/11/10 | No Sample | 0.4 | 0.4 | 0 | 0 | 0 | 0 | 0.00 % | 0.00 % | 0.00 % | 3 | 1.2 | 6.53 | 5.44 | |
| 2015/11/10 | 3 Discs | 0.4 | 0.4 | 0 | 0 | 0 | 0 | 0.00 % | 0.00 % | 0.00 % | 3 | 1.2 | 0.64 | 0.54 | 6.17 |
| 2015/11/10 | 3 Discs | 0.4 | 0.4 | 0 | 0 | 0 | 0 | 0.00 % | 0.00 % | 0.00 % | 3 | 1.2 | 2.95 | 2.46 | 3.86 |

Table 8 shows test data of Round-2 under inlet gas stream conditions of nitrogen flow only, at ambient temperature (59 $^oF$ ). When the disks were not placed in the chamber, the detected $Hg^0$ concentrations at the outlet of the chamber were 5.89 ng/L, 5.61 ng/L, 5.77 ng/L and 5.44 ng/L. After the synthetic disks were put into the chamber, $Hg^0$ concentrations were detected as: 0.54ng/L and 2.46 ng/L. The $Hg^0$ capturing capacity of the disks led to the difference of $Hg^0$ concentration in the gas stream.

Table 9: Test Result for 100% $N_2$ Gas Experiment (Round 2, 100 $^oF$ )

| Round-2-2 | | | | | | | | | | | | | | | |
|---|---|---|---|---|---|---|---|---|---|---|---|---|---|---|---|
| Date | Sample Discs in the Chamber | Total Flow | Flowmeter 1 | Flowmeter 2 | Flowmeter 3 | Simulated Flue Gas Components | | | | | Flow Sampling Time | Total Sampling Volume | PSA Measurement Value | Hg Concentration in Sample | Absorption |
| | | | N2+Hg | SO2 (4%) + NO (2%) + N2 (balance) | CO2 (25%) + O2 (10%) + N2 (balance) | SO2 | NO | CO2 | O2 | N2 | | | | | |
| | | L/min | L/min | L/min | L/min | ppm | ppm | % | % | % | min | L | ng | ng/L | ng |
| 2015/11/23 | No Sample | 0.4 | 0.4 | 0 | 0 | 0 | 0 | 0.00 % | 0.00 % | 0.00 % | 3 | 1.2 | 6.76 | 5.63 | |
| 2015/11/23 | No Sample | 0.4 | 0.4 | 0 | 0 | 0 | 0 | 0.00 % | 0.00 % | 0.00 % | 3 | 1.2 | 7.09 | 5.91 | |
| 2015/11/23 | No Sample | 0.4 | 0.4 | 0 | 0 | 0 | 0 | 0.00 % | 0.00 % | 0.00 % | 3 | 1.2 | 6.74 | 5.62 | |
| 2015/11/23 | No Sample | 0.4 | 0.4 | 0 | 0 | 0 | 0 | 0.00 % | 0.00 % | 0.00 % | 3 | 1.2 | 6.75 | 5.63 | |
| 2015/11/23 | 3 Discs | 0.4 | 0.4 | 0 | 0 | 0 | 0 | 0.00 % | 0.00 % | 0.00 % | 3 | 1.2 | 1.24 | 1.04 | 5.59 |
| 2015/11/23 | 3 Discs | 0.4 | 0.4 | 0 | 0 | 0 | 0 | 0.00 % | 0.00 % | 0.00 % | 3 | 1.2 | 3.46 | 2.88 | 3.38 |

Table 9 shows test data of Round-2 under inlet gas stream conditions of nitrogen flow only, at 100°F. When the disks were not placed in the chamber, the detected $Hg^0$ concentrations at the outlet of the chamber were 5.63 ng/L, 5.91 ng/L, 5.62 ng/L and 5.63 ng/L. After the synthetic disks were put into the chamber, $Hg^0$ concentrations were detected as: 1.04ng/L and 2.88 ng/L. The $Hg^0$ capturing capacity of the disks led to the difference of $Hg^0$ concentration in the gas stream.

Table 10: Test Result for 100% $N_2$ Gas Experiment (Round 2, $150^oF$ )

| Round-2-3 | | | | | | | | | | | | | | | |
|---|---|---|---|---|---|---|---|---|---|---|---|---|---|---|---|
| Date | Sample Discs in the Chamber | Total Flow | Flowmeter 1 | Flowmeter 2 | Flowmeter 3 | Simulated Flue Gas Components | | | | | Flow Sampling Time | Total Sampling Volume | PSA Measurement Value | Hg Concentration in Sample Gas | Absorption |
| | | | N2+Hg | SO2 (4%) + NO (2%) + N2 (balance) | CO2 (25%) + O2 (10%) + N2 (balance) | SO2 | NO | CO2 | O2 | N2 | | | | | |
| | | L/min | L/min | L/min | L/min | ppm | ppm | % | % | % | min | L | ng | ng/L | ng |
| 2015/11/26 | No Sample | 0.4 | 0.4 | 0 | 0 | 0 | 0 | 0.00 % | 0.00 % | 0.00 % | 3 | 1.2 | 4.86 | 4.05 | |
| 2015/11/26 | No Sample | 0.4 | 0.4 | 0 | 0 | 0 | 0 | 0.00 % | 0.00 % | 0.00 % | 3 | 1.2 | 4.66 | 3.89 | |
| 2015/11/26 | No Sample | 0.4 | 0.4 | 0 | 0 | 0 | 0 | 0.00 % | 0.00 % | 0.00 % | 3 | 1.2 | 4.95 | 4.12 | |
| 2015/11/26 | No Sample | 0.4 | 0.4 | 0 | 0 | 0 | 0 | 0.00 % | 0.00 % | 0.00 % | 3 | 1.2 | 4.61 | 3.84 | |
| 2015/11/26 | 3 Discs | 0.4 | 0.4 | 0 | 0 | 0 | 0 | 0.00 % | 0.00 % | 0.00 % | 3 | 1.2 | 0.86 | 0.72 | 3.91 |
| 2015/11/26 | 3 Discs | 0.4 | 0.4 | 0 | 0 | 0 | 0 | 0.00 % | 0.00 % | 0.00 % | 3 | 1.2 | 2.91 | 2.43 | 1.86 |

Table 10 shows test data of Round-2 under inlet gas stream conditions of nitrogen flow only, at 150°F. When the disks were not placed in the chamber, the detected $Hg^0$ concentrations at the outlet of the chamber were 4.05 ng/L, 3.89 ng/L, 4.12 ng/L and 3.84 ng/L. After the synthetic disks were put into the chamber, $Hg^0$ concentrations were detected as: 0.72ng/L and 2.43 ng/L. The $Hg^0$ capturing capacity of the disks led to the difference of $Hg^0$ concentration in the gas stream.

Table 11: Test Result for 100% $N_2$ Gas Experiment (Round 2, 200 $^{\circ}F$ )

| Round-2-4 | | | | | | | | | | | | | | | |
|---|---|---|---|---|---|---|---|---|---|---|---|---|---|---|---|
| Date | Sample Discs in the Chamber | Total Flow | Flowmeter 1 | Flowmeter 2 | Flowmeter 3 | Simulated Flue Gas Components | | | | | Flow Sampling Time | Total Sampling Volume | PSA Measurement Value | Hg Concentration in Sample Gas | Absorption |
| | | | N2+Hg | SO2 (4%) + NO (2%) + N2(balance) | CO2 (25%) + O2 (10%) + N2(balance) | SO2 | NO | CO2 | O2 | N2 | | | | | |
| | | L/min | L/min | L/min | L/min | ppm | ppm | % | % | % | min | L | ng | ng/L | ng |
| 2015/11/29 | No Sample | 0.4 | 0.4 | 0 | 0 | 0 | 0 | 0.0% | 0.0% | 0.0% | 3 | 1.2 | 6.17 | 5.14 | |
| 2015/11/29 | No Sample | 0.4 | 0.4 | 0 | 0 | 0 | 0 | 0.0% | 0.0% | 0.0% | 3 | 1.2 | 6.12 | 5.10 | |
| 2015/11/29 | No Sample | 0.4 | 0.4 | 0 | 0 | 0 | 0 | 0.0% | 0.0% | 0.0% | 3 | 1.2 | 6.15 | 5.12 | |
| 2015/11/29 | No Sample | 0.4 | 0.4 | 0 | 0 | 0 | 0 | 0.0% | 0.0% | 0.0% | 3 | 1.2 | 5.72 | 4.76 | |
| 2015/11/29 | 3 Discs | 0.4 | 0.4 | 0 | 0 | 0 | 0 | 0.0% | 0.0% | 0.0% | 3 | 1.2 | 2.84 | 2.37 | 3.20 |
| 2015/11/29 | 3 Discs | 0.4 | 0.4 | 0 | 0 | 0 | 0 | 0.0% | 0.0% | 0.0% | 3 | 1.2 | 2.73 | 2.28 | 3.31 |

Table 4 shows test data of Round-2 under inlet gas stream conditions of nitrogen flow only, at 200°F. When the disks were not placed in the chamber, the detected $Hg^0$ concentrations at the outlet of the chamber were 5.14 ng/L, 5.10 ng/L, 5.12 ng/L and 4.76 ng/L. After the synthetic disks were put into the chamber, $Hg^0$ concentrations were detected as: 2.37ng/L and 2.28 ng/L. The $Hg^0$ capturing capacity of the disks led to the difference of $Hg^0$ concentration in the gas stream.

Table 12: Test Results for 100% $N_2$ Gas Experiment

| Number of the test | Hg Concentration in Flue Average | Total Hg Absorbed | Flue Gas Temperature | Flue Gas Temperature | Number of Discs | Disc Diameter | Calculated Average Hg Concentration on Each Disc | Calculated Average Hg on Each Disc | Efficiency |
|---|---|---|---|---|---|---|---|---|---|
| | ng/L | ng | Deg. C | ° F | | cm | ng/cm^2 | ng | % |
| Round 1-1 | 5.89 | 11.52 | 20 | 68 | 3 | 2.22 | 0.99 | 3.84 | 44.42 |
| Round 1-2 | 6.13 | 26.89 | 37 | 98.6 | 3 | 2.22 | 2.32 | 8.96 | 91.37 |
| Round 1-3 | 9.65 | 32.19 | 67 | 152.6 | 3 | 2.22 | 2.77 | 10.73 | 49.07 |
| Round 1-4 | 34.46 | 189.46 | 93 | 199.4 | 3 | 2.22 | 16.32 | 63.15 | 91.63 |
| Round 2-1 | 5.68 | 36.79 | 15 | 59 | 3 | 2.22 | 3.17 | 12.26 | 73.61 |
| Round 2-2 | 5.7 | 37.39 | 37 | 98.6 | 3 | 2.22 | 3.22 | 12.46 | 65.63 |
| Round 2-3 | 3.98 | 21.16 | 66 | 150.8 | 3 | 2.22 | 1.82 | 7.05 | 60.49 |
| Round 2-4 | 5.03 | 32.53 | 92 | 197.6 | 3 | 2.22 | 2.8 | 10.84 | 53.86 |

The $Hg^0$ absorption efficiency of the synthetic disks and the mass of $Hg^0$ absorbed on each disk were computed as Table 12. The results show that in Round-1, the $Hg^0$ absorption efficiency was randomly affected by the burnt edge of the synthetic disks. In Round-2, the $Hg^0$ absorption efficiency of the synthetic disks was monotonically decreasing (73.61%, 65.63%, 60.49% and 53.86%) with the increased inlet flue gas temperature (59°F, 98.6°F, 150.8°F and 197.6°F).

Curves of inlet gas temperature vs. Hg° absorption efficiency are shown in Figure 15. The blue line shows the Hg° absorption efficiency for the synthetic disks in Round-1 testing and the red line compared to the Hg° absorption efficiency of the disks in Round-2. Because of the burnt edge of the synthetic disks, the Hg° absorption efficiency of the disks in Round-1 was not consistence with the inlet gas temperature. The red line, which was the result of Round-2, decreases monotonically with increasing of the inlet gas temperature. Therefore, the results of Round-2 were used throughout the later sections of this study to represent the Hg° absorption efficiency of the disks in nitrogen flow at different temperature levels and the results of Round-1 were discarded.

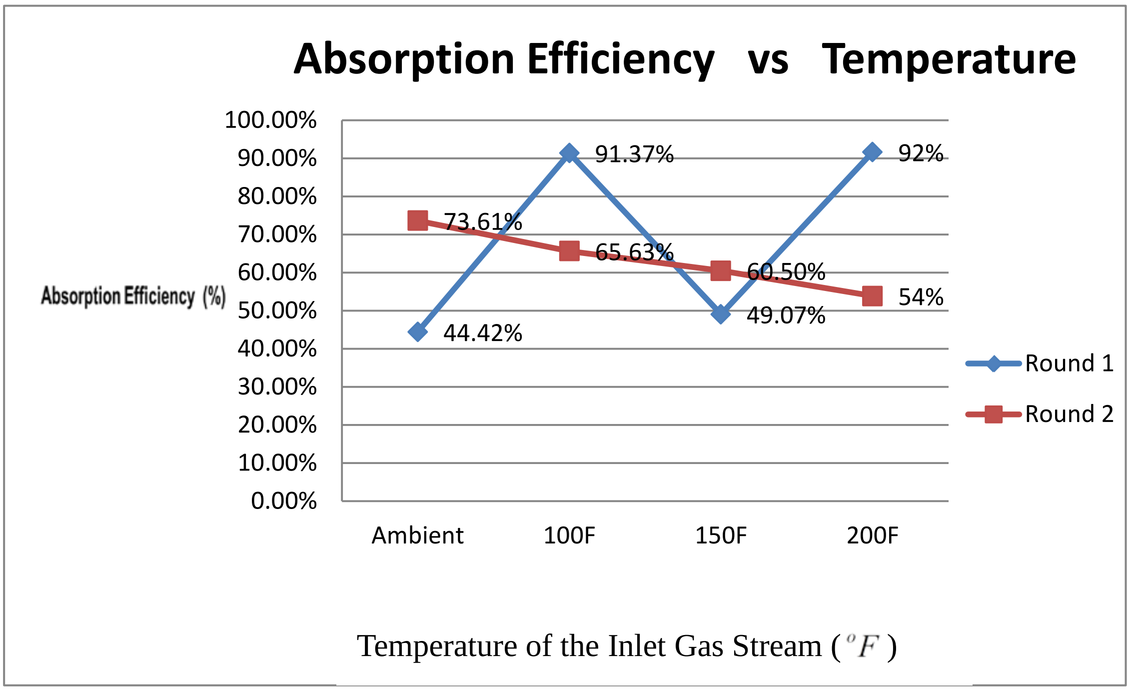


Figure 15: Hg° Absorption Efficiency Curve of Round 1 and Round 2

### 4.1.2 Simulation Results

The objective of the CFD simulations of the temperature field in the chamber was to provide a more realistic value of the gas temperature at the disc locations in the chamber. The simulations ran in FLUENT software, used the pressure-based solver with absolute velocity and steady time formulation. A laminar viscous flow was assumed in the model. The material used as wall material was stainless steel from the FLUENT database and the flow was assumed to be nitrogen, of which the properties are shown in Table 13 [9].

Table 13: Gas Properties of $N_2$

| Inlet Gas Temperature | 310K ( 37 $^oC$ ) | 339K ( 66 $^oC$ ) | 365K ( 92 $^oC$ ) |
|---|---|---|---|
| Density (kg/ $m^3$) | 1.100468 | 1.005959 | 0.935478 |
| Thermal Conductivity (W/m-K) | 0.02802 | 0.02992 | 0.03165 |
| Viscosity (kg/m-s) | 0.00162 | 0.00199 | 0.0021 |
| Specific Heat (J/kg-K) | 1038.745 | 1041.675 | 1044.606 |

The type of the inlet flow was set as velocity inlet. The velocity of the inlet gas stream was calculated with the known total flow rate and inlet cross section area.

The inlet gas temperature was measured by a thermocouple. The wall temperature, which was the temperature of the chamber internal surface, was detected by a thermocouple placed inside the chamber. The chamber was well insulated with asbestos.The convective heat coefficient of the wall was assumed to be $1W/m^2*K$ [8]. Simple scheme was applied as pressure-velocity coupling and spatial discretization was set as least square cell based gradient, second order pressure, second order upwind momentum and second order upwind energy. Standard initialization method was applied. Simulation results were shown below.

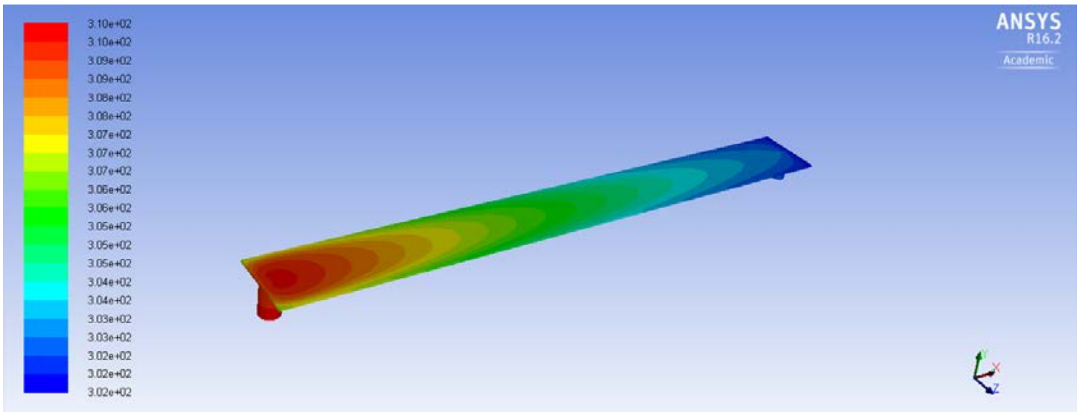


Figure 16: Temperature Field of the Chamber, $N_2$ , 100 $^oF$

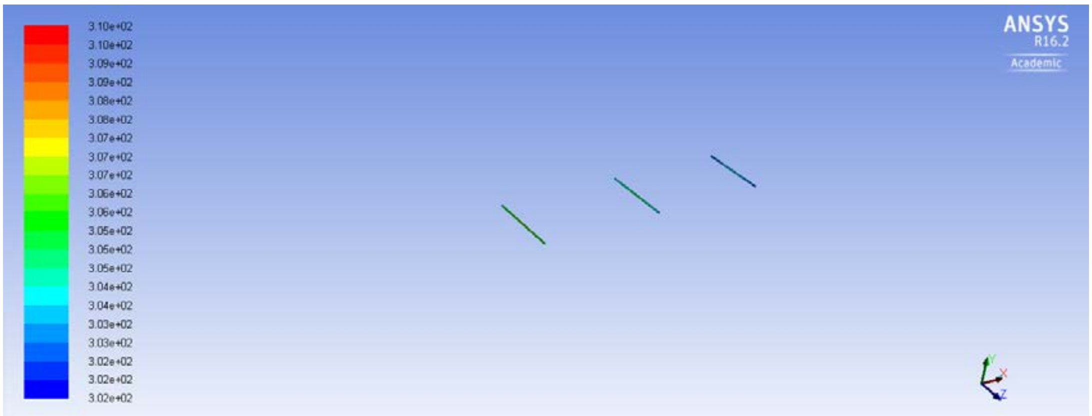


Figure 17: Temperature Display of the Center Disk Positions, $N_2$ , 100 $^oF$

Figure 16 shows the simulated temperature field inside the chamber under a condition of nitrogen flow at 100°F, the gas temperature decreases from the inlet port to the outlet port. Three disks were placed in the chamber. The three color bars in Figure 17 indicate the gas temperature at the center of the disk locations in the chamber: 306K, 305K and 304K. An average temperature of 305K at three disk locations was used as the temperature value of the gas temperature at the disk positions in the chamber.

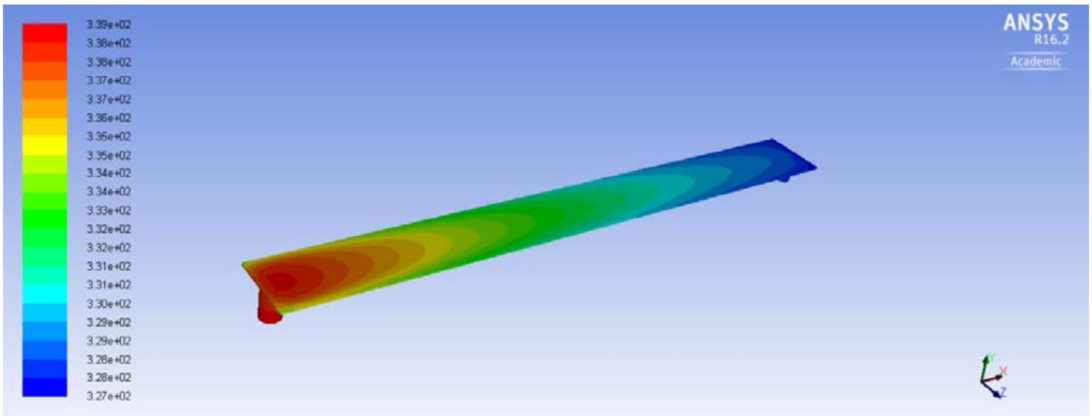


Figure 18: Temperature Field of the Chamber, $N_2$ , 150 $^oF$

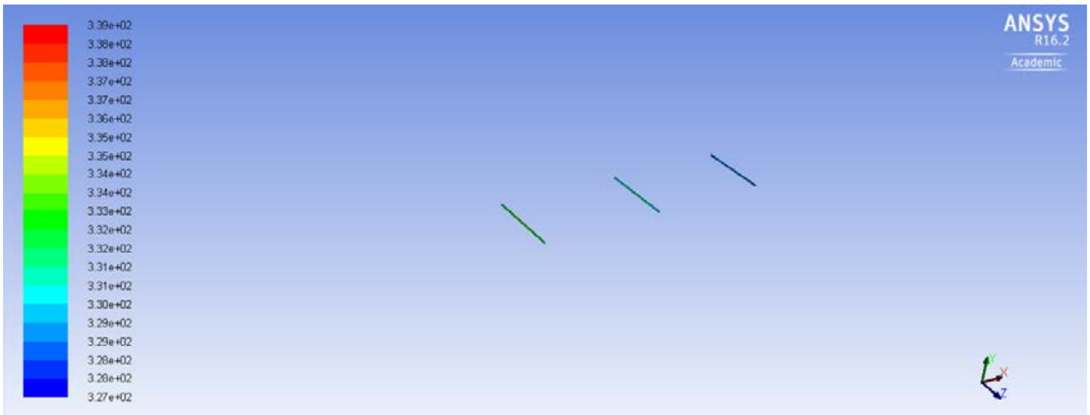


Figure 19: Temperature Display of the Center Disk Position, $N_2$ , 150 $^oF$

Figure 18 shows the simulated temperature field inside the chamber under a condition of nitrogen flow at 150°F, the gas temperature decreases from the inlet port to the outlet port. Three disks were placed in the chamber. The three color bars in Figure 19 indicate the gas temperature at the center of the disk positions: 332K, 331K and 330K. An average temperature of 331K at three disk positions was used as the temperature value of the gas temperature at the disk positions in the chamber.

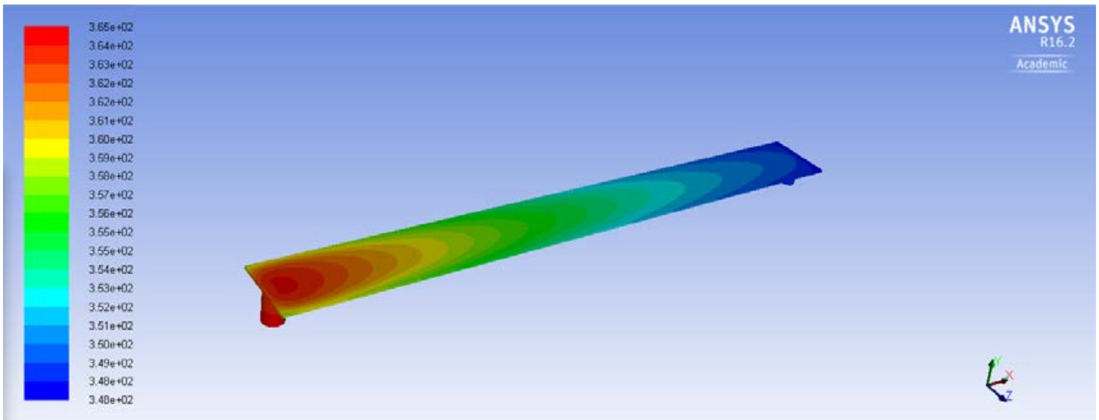


Figure 20: Temperature Field of the Chamber, $N_2$ , 200 $^{o}F$

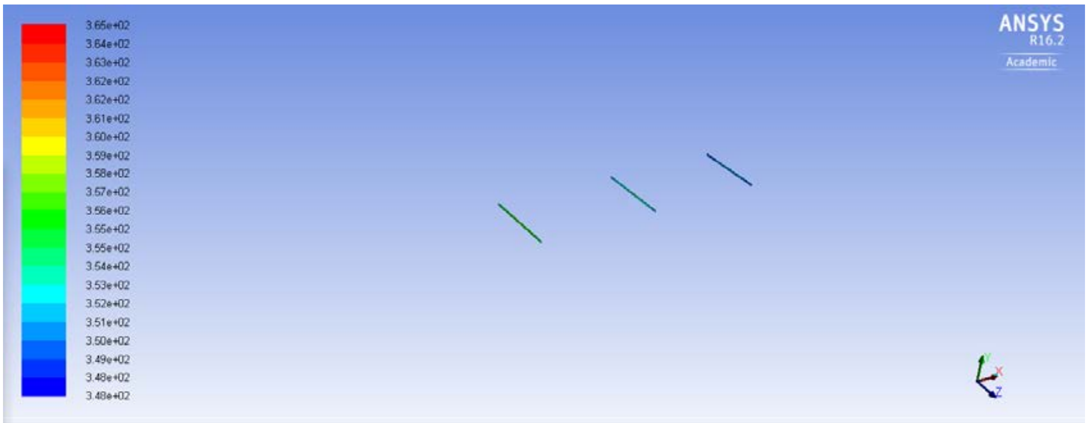


Figure 21: Temperature Display of the Center Disk Position, $N_2$ , 200 $^{o}F$

Figure 20 shows the simulated temperature field inside the chamber under a condition of nitrogen flow at 200°F, gas temperature decreases from the inlet port to the outlet port. Three disks were placed in the chamber. The three color bars in Figure 21 indicate the gas temperature at the center of the disk positions: 356K, 354K and 352K. An average temperature of 331K at three disk positions was used as the temperature value of the gas temperature at the disk positions in the chamber.

The average temperature of the gas stream at the three disk positions and the measured inlet gas temperature are listed in Table 14.

Table 14: Inlet Gas Temperature and Simulated Gas Temperature

| | | | |
|---|---|---|---|
| Inlet gas temperature (K) | 310 | 339 | 365 |
| Simulated gas temperature (K) | 305 | 331 | 354 |
| Simulated gas temperature ($^oF$) | 89.6 | 136.4 | 177.8 |

The inlet gas temperature, used in the $Hg^0$ absorption efficiency curve, was replaced by the simulated gas temperature at the disk positions. A fitting curve of the $Hg^0$ absorption efficiency vs. gas temperature at disk positions is plotted in Figure 22.

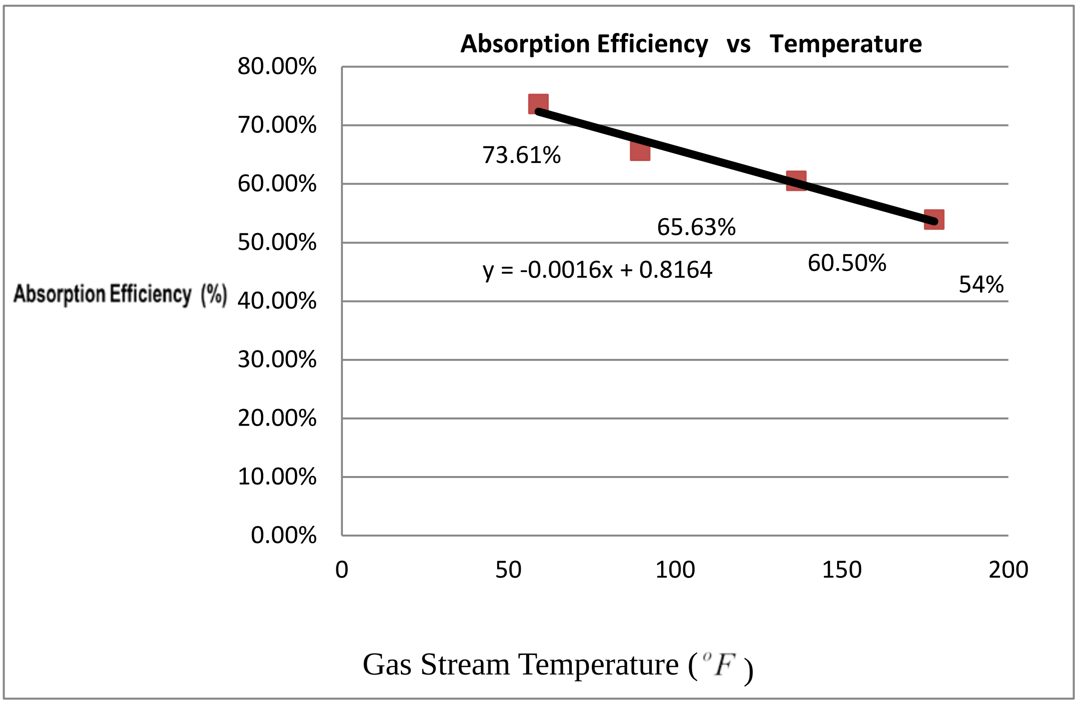


Figure 22: $Hg^0$ Absorption Efficiency vs. Temperature (in $N_2$ Flow)

## 4.2 Case-2: Simulated Flue Gas

Four groups of tests were run under a gas mixture composed of 700 ppm NO, 350 ppm $SO_2$, 12.5% $CO_2$, 5% $O_2$ and $N_2$ as the balance gas to determine the $Hg^0$ absorption capacity of synthetic disks in a more realistic simulated flue gas. The $Hg^0$ concentration was set at 5 ng/ L to simulate a low mercury emissions level in the test gas. Because of the problem in Round-1, where the edge of the synthetic disks was burnt by the heater in the chamber, in these experiments, the heater was not turned on. Thus, in the simulated flue gas testing, there were three temperature levels (ambient temperature, $100\,^oF$ and $150\,^oF$) used in the experiment.

Tables 15, 16 and 17 show the test results of $Hg^0$ absorption of the synthetic disks at ambient temperature, $100\,^oF$ and $150\,^oF$.

## 4.2.1 Test Results

Table 15: Test Result for Mixture Gas Experiment (Ambient Temperature, 59 $^oF$ )

| Date | Sample Discs in the Chamber | Total Flow | Flowmeter 1 | Flowmeter 2 | Flowmeter 3 | Simulated Flue Gas Components | | | | | Flow Sampling Time | Total Sampling Volume | PSA Measurement Value | Hg Concentration in Sample Gas | Absorption |
|---|---|---|---|---|---|---|---|---|---|---|---|---|---|---|---|
| | | | $N_2$+Hg | $SO_2$ (4%) + NO (2%) + $N_2$(balance) | $CO_2$ (25%) + $O_2$ (10%) + $N_2$(balance) | $SO_2$ | NO | $CO_2$ | $O_2$ | $N_2$ | | | | | |
| | | L/min | L/min | L/min | L/min | ppm | ppm | % | % | % | min | L | ng | ng/L | ng |
| 2015/12/27 | No Sample | 0.82 | 0.4 | 0.02 | 0.4 | 976 | 488 | 12.20% | 4.88% | 82.78% | 3 | 2.46 | 14.24 | 5.79 | |
| 2015/12/27 | No Sample | 0.82 | 0.4 | 0.02 | 0.4 | 976 | 488 | 12.20% | 4.88% | 82.78% | 3 | 2.46 | 15.02 | 6.11 | |
| 2015/12/27 | No Sample | 0.82 | 0.4 | 0.02 | 0.4 | 976 | 488 | 12.20% | 4.88% | 82.78% | 3 | 2.46 | 15.24 | 6.19 | |
| 2015/12/27 | No Sample | 0.82 | 0.4 | 0.02 | 0.4 | 976 | 488 | 12.20% | 4.88% | 82.78% | 3 | 2.46 | 14.58 | 5.93 | |
| 2015/12/27 | 3 Discs | 0.82 | 0.4 | 0.02 | 0.4 | 976 | 488 | 12.20% | 4.88% | 82.78% | 3 | 2.46 | 0.44 | 0.18 | 14.33 |
| 2015/12/27 | 3 Discs | 0.82 | 0.4 | 0.02 | 0.4 | 976 | 488 | 12.20% | 4.88% | 82.78% | 3 | 2.46 | 0.71 | 0.29 | 14.06 |

Table 16: Test Result for Mixture Gas Experiment (100 °$F$ )

| Date | Sample Discs in the Chamber | Total Flow | Flowmeter 1 | Flowmeter 2 | Flowmeter 3 | Simulated Flue Gas Components | | | | | Flow Sampling Time | Total Sampling Volume | PSA Measurement Value | Hg Concentration in Sample Gas | Absorption |
|---|---|---|---|---|---|---|---|---|---|---|---|---|---|---|---|
| | | | $N_2$+Hg | $SO_2$ (2%) + NO (4%) + $N_2$(balance) | $CO_2$ (25%) + $O_2$ (10%) + $N_2$(balance) | $SO_2$ | NO | $CO_2$ | $O_2$ | $N_2$ | | | | | |
| | | L/min | L/min | L/min | L/min | ppm | ppm | % | % | % | min | L | ng | ng/L | ng |
| 2016/3/10 | No Sample | 0.51 | 0.25 | 0.01 | 0.25 | 392 | 784 | 12.25% | 4.90% | 82.76% | 3 | 1.53 | 6.36 | 4.16 | |
| 2016/3/10 | No Sample | 0.51 | 0.25 | 0.01 | 0.25 | 392 | 784 | 12.25% | 4.90% | 82.76% | 3 | 1.53 | 6.90 | 4.51 | |
| 2016/3/10 | No Sample | 0.51 | 0.25 | 0.01 | 0.25 | 392 | 784 | 12.25% | 4.90% | 82.76% | 3 | 1.53 | 6.59 | 4.31 | |
| 2016/3/10 | No Sample | 0.51 | 0.25 | 0.01 | 0.25 | 392 | 784 | 12.25% | 4.90% | 82.76% | 3 | 1.53 | 6.21 | 4.06 | |
| 2016/3/10 | 3 Discs | 0.51 | 0.25 | 0.01 | 0.25 | 392 | 784 | 12.25% | 4.90% | 82.76% | 3 | 1.53 | 1.90 | 1.24 | 4.62 |
| 2016/3/10 | 3 Discs | 0.51 | 0.25 | 0.01 | 0.25 | 392 | 784 | 12.25% | 4.90% | 82.76% | 3 | 1.53 | 3.02 | 1.97 | 3.50 |
| 2016/3/10 | 3 Discs | 0.51 | 0.25 | 0.01 | 0.25 | 392 | 784 | 12.25% | 4.90% | 82.76% | 3 | 1.53 | 2.75 | 1.80 | 3.76 |

Table 17: Test Result for Mixture Gas Experiment ($150\,^{o}F$)

| Date | Sample Discs in the Chamber | Total Flow | Flowmeter 1 | Flowmeter 2 | Flowmeter 3 | Simulated Flue Gas Components | | | | | Flow Sampling Time | Total Sampling Volume | PSA Measurement Value | Hg Concentration in Sample Gas | Absorption |
|---|---|---|---|---|---|---|---|---|---|---|---|---|---|---|---|
| | | | N2+Hg | SO2 (2%) + NO (4%) + N2(balance) | CO2 (25%) + O2 (10%) + N2(balance) | SO2 | NO | CO2 | O2 | N2 | | | | | |
| | | L/min | L/min | L/min | L/min | ppm | ppm | % | % | % | min | L | ng | ng/L | ng |
| 2016/3/11 | No Sample | 0.815 | 0.4 | 0.015 | 0.4 | 368 | 736 | 12.27% | 4.91% | 82.75% | 3 | 2.445 | 11.03 | 4.51 | |
| 2016/3/11 | No Sample | 0.815 | 0.4 | 0.015 | 0.4 | 368 | 736 | 12.27% | 4.91% | 82.75% | 3 | 2.445 | 11.21 | 4.59 | |
| 2016/3/11 | No Sample | 0.815 | 0.4 | 0.015 | 0.4 | 368 | 736 | 12.27% | 4.91% | 82.75% | 3 | 2.445 | 10.62 | 4.35 | |
| 2016/3/11 | No Sample | 0.815 | 0.4 | 0.015 | 0.4 | 368 | 736 | 12.27% | 4.91% | 82.75% | 3 | 2.445 | 10.43 | 4.27 | |
| 2016/3/11 | No Sample | 0.815 | 0.4 | 0.015 | 0.4 | 368 | 736 | 12.27% | 4.91% | 82.75% | 3 | 2.445 | 10.50 | 4.30 | |
| 2016/3/11 | No Sample | 0.815 | 0.4 | 0.015 | 0.4 | 368 | 736 | 12.27% | 4.91% | 82.75% | 3 | 2.445 | 10.46 | 4.28 | |
| 2016/3/11 | 3 Discs | 0.815 | 0.4 | 0.015 | 0.4 | 368 | 736 | 12.27% | 4.91% | 82.75% | 3 | 2.445 | 7.74 | 3.17 | 2.97 |
| 2016/3/11 | 3 Discs | 0.815 | 0.4 | 0.015 | 0.4 | 368 | 736 | 12.27% | 4.91% | 82.75% | 3 | 2.445 | 5.89 | 2.41 | 4.82 |

Table 18: Test Results for the Mixture Gas Experiment

| Number of the test | Hg Concentration in Flue Average | Total Hg Absorbed | Flue Temperature | Flue Temperature | Number of Discs | Disc Diameter | Calculated Average Hg Concentration on Disc | Calculated Average Hg on Disc | Efficiency |
|---|---|---|---|---|---|---|---|---|---|
| | ng/L | ng | Deg. C | ° F | | cm | ng/cm^2 | ng | % |
| 1 | 6.00 | 104.09 | 15 | 59 | 3 | 2.22 | 8.97 | 34.7 | 96.1 |
| 2 | 4.26 | 31.68 | 37 | 98.6 | 3 | 2.22 | 2.73 | 10.56 | 60.78 |
| 3 | 4.38 | 28057 | 65 | 149 | 3 | 2.22 | 2.46 | 9.52 | 36.37 |

The $Hg^0$ absorption efficiency of the synthetic disks and the mass of $Hg^0$ absorbed on each disk were computed as Table 18. The $Hg^0$ absorption efficiency of the synthetic disks was monotonically decreasing (96.1%, 60.78% and 36.37%) with the increased inlet flue gas temperature (59°F, 98.6°F and 149°F).

The curve of inlet gas temperature vs. $Hg^0$ absorption efficiency is shown in Figure 23. The plot indicates the result of the tests with a gas mixture at different temperature levels. The $Hg^0$ absorption efficiency decreases from approximate 96.1% at 59°F to about 36.37% at 150°F.

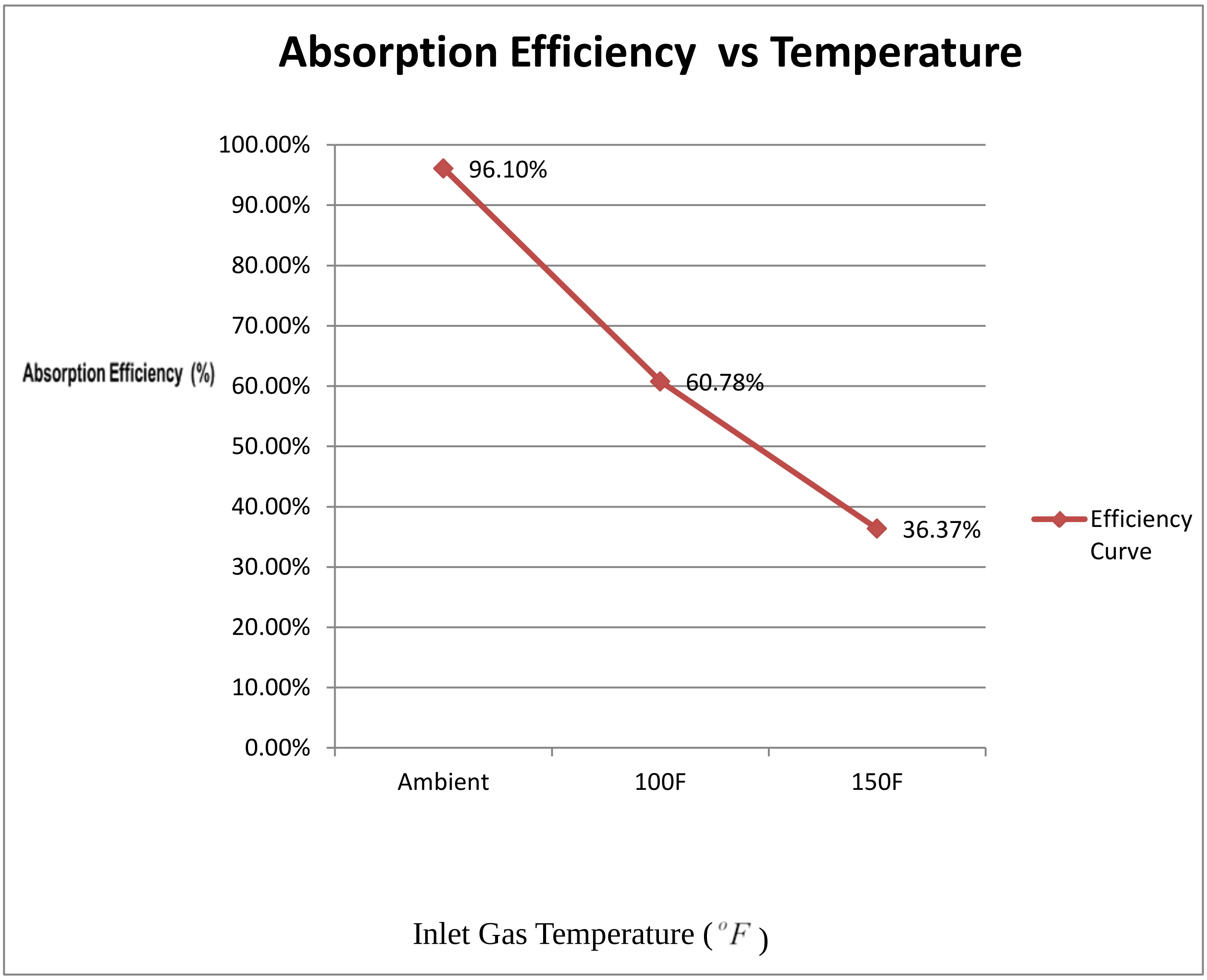


Figure 23: $Hg^0$ Absorption Efficiency vs. Inlet Gas Temperature

### 4.2.2 Simulation Results

The simulation models and assumptions were set the same as Case-1. The material used as the wall material was assumed to be stainless steel from the FLUENT database and the flow material was assumed to be stack gas, of which the properties were shown in Table 19 [9].

Table 19: Properties of the Simulated Flue Gas

| Inlet Gas Temperature | 310K ( 37 $^oC$ ) | 338K ( 65 $^oC$ ) |
|---|---|---|
| Density (kg/ $m^3$) | 1.186968 | 1.089256 |
| Thermal Conductivity (W/m-K) | 0.02646 | 0.02827 |
| Viscosity (kg/m-s) | 0.00184 | 0.00197 |
| Specific Heat (J/kg-K) | 999.389 | 1006.506 |

The inlet gas stream velocity was calculated based on the total flow rate, which was measured in this case. Inlet gas temperature was measured by a thermocouple and the wall temperature, which represented the temperature of the chamber internal surface, was detected by a thermocouple placed inside the chamber. Other settings were similar to Case-1. Simulation results were shown below.

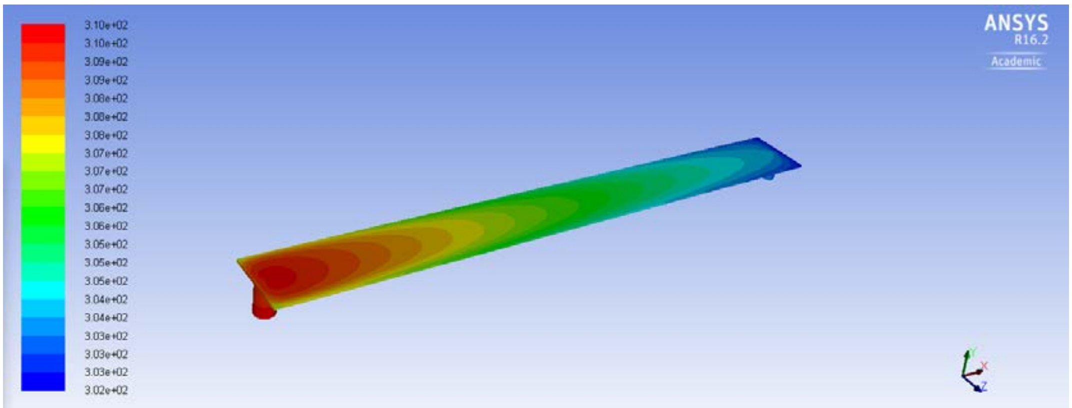


Figure 24: Temperature Field of the Chamber, Mixture gas, 100 $^oF$

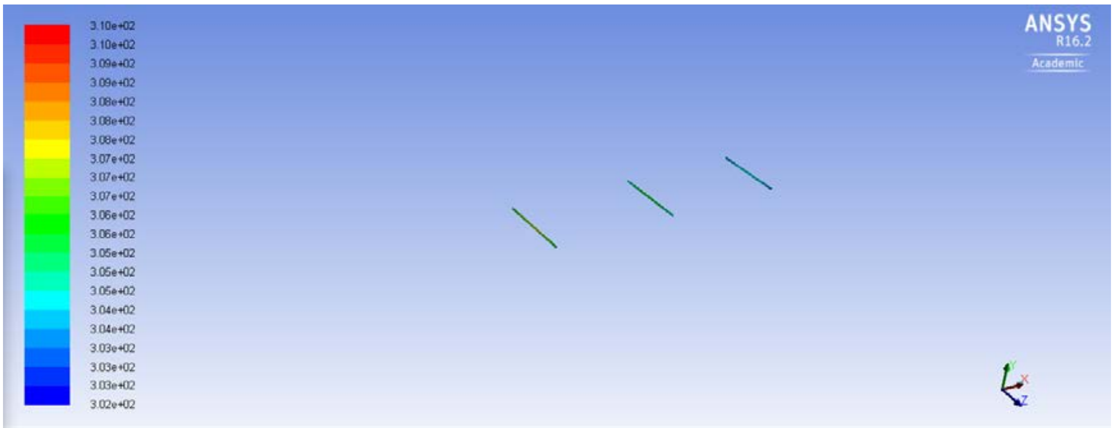


Figure 25: Temperature Display of the Center Disk Position, Mixture gas, 100 $^oF$

Figure 24 shows the simulated temperature field inside the chamber under a condition of mixture gas flow at 100°F, the gas temperature decreases from the inlet port to the outlet port. Three disks were placed in the chamber. The three color bars in Figure 25 indicate the gas temperature at the center of the disk positions: 306K, 305K and 304K. An average temperature of 305K at three disk positions was used as the temperature value of the gas temperature at the disk positions in the chamber.

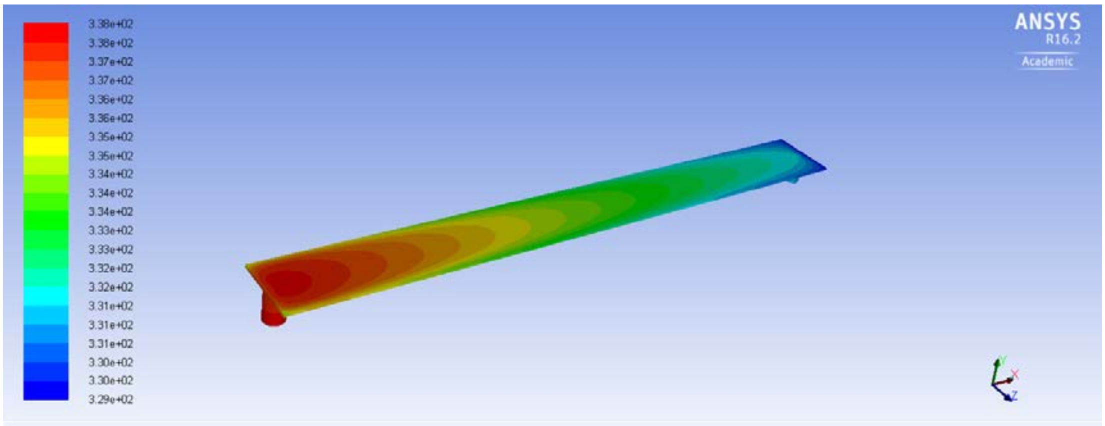


Figure 26: Temperature Field of the Chamber, Mixture gas, 150 $^{o}F$

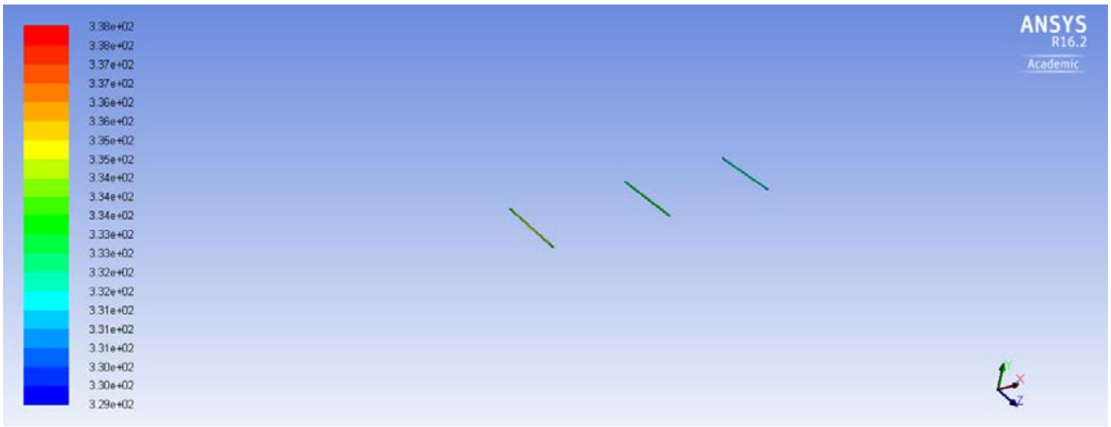


Figure 27: Temperature Display of the Center Disk Position, Mixture gas, 150 $^{o}F$

Figure 26 shows the simulated temperature field inside the chamber under a condition of mixture gas flow at 150°F, the gas temperature decreases from the inlet port to the outlet port. Three disks were placed in the chamber. The three color bars in Figure 27 indicate the gas temperature at the center of the disk positions: 334K, 332K and 330K. An average temperature of 332K at three disk positions was used as the temperature value of the gas temperature at the disk positions in the chamber.

The average temperature of the gas stream at the three disk positions and the measured inlet gas temperature are listed in Table 20. The temperature difference between the inlet gas temperature of 310K and the simulated gas temperature (305K) was 5K, the same as that in 100% nitrogen flow at same inlet temperature level. However, in simulated flue gas tests at the inlet gas temperature level of 339K, the temperature difference was 7K, compared to the temperature difference of 8K in 100% nitrogen flow at same inlet temperature level.

Table 20: Inlet Gas Temperature and Simulated Gas Temperature

| | | |
|---|---|---|
| Inlet gas temperature (K) | 310 | 339 |
| Simulated gas temperature (K) | 305 | 332 |
| Simulated gas temperature ($^oF$) | 89.6 | 138.2 |

The inlet gas temperature, used in the $Hg^0$ absorption efficiency curve, was replaced by the simulated gas temperature at the disk positions. A fitting curve of the $Hg^0$ absorption efficiency vs. gas temperature at disk positions is plotted in Figure 28.

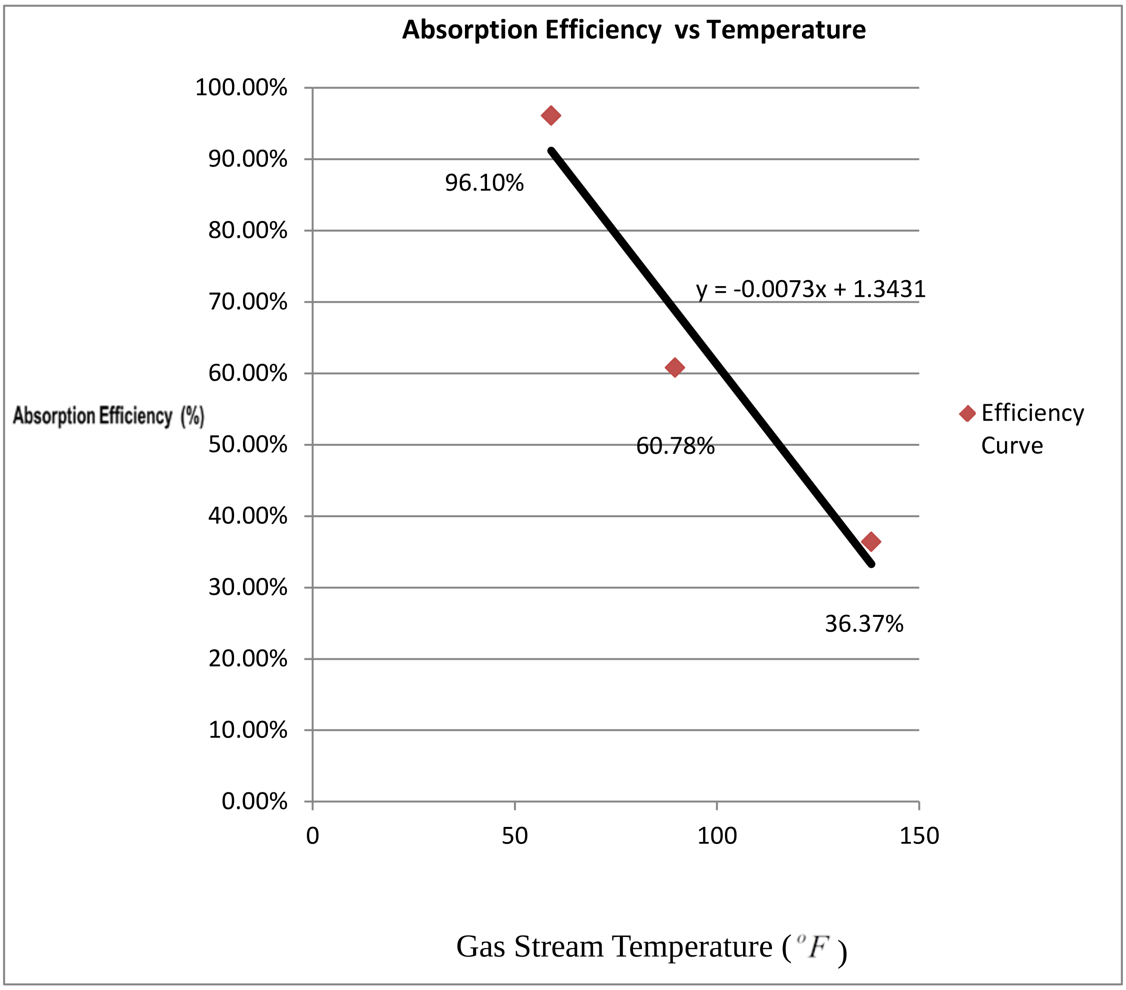


Figure 28: $Hg^0$ Absorption Efficiency Curve vs. Temperature (in Simulated Flue)

## 4.3 Case-3: Simulated Flue Gas with Moisture

A group of tests to determine the impact of moisture on the $Hg^0$ absorption ability of the synthetic disks performed with the mixture of gas used in Case-2. The moisture level of flow was controlled at 20% and the inlet gas temperature was set at 150°F, to simulate the condition of the flue gas after a wet desulfurization system.

The flow condition for this experiment was given in Table 21.

Table 21: Flow Conditions in Humidity Calculation

| Flow component | $N_2$ | $CO_2 + O_2 + N_2$ | $SO_2$ +NO+ $N_2$ | $H_2O$ |
|---|---|---|---|---|
| Flow rate | 300 ml/min | 300 ml/min | 12 ml/min | 2.4/14 ml/min |

The mass flow rater of the overall gas stream was 0.762 g/min and the mass flow rate of water was calculated:

2.5(ml) * 1(g/ml) / 14min= 0.1786 g/min (6)

Therefore, the moisture level in the gas stream was:

0.1786 / (0.762+0.1786) = 18.988% (7)

Test results are given in Table 22.

Table 22: Test Result for Mixture Gas Experiment with Moisture (150 °F)

| Date | Sample Discs in the Chamber | Total Flow | Flowmeter 1 | Flowmeter 2 | Flowmeter 3 | Simulated Flue Gas Components | | | | | | Flow Sampling Time | Total Sampling Volume | PSA Measurement Value | Hg Concentration in Sample Gas | Absorption |
|---|---|---|---|---|---|---|---|---|---|---|---|---|---|---|---|---|
| | | | N2+Hg | SO2 (2%) + NO (4%) + N2(balance) | CO2 (25%) + O2 (10%) + N2(balance) | SO2 | NO | CO2 | O2 | N2 | H2O | | | | | |
| | | L/min | L/min | L/min | L/min | ppm | ppm | % | % | % | % | min | L | ng | ng/L | ng |
| 2016/4/5 | No Sample | 0.612 | 0.3 | 0.012 | 0.3 | 392 | 784 | 12.25% | 4.90% | 82.76% | 18.998% | 3 | 1.836 | 17.73 | 9.66 | |
| 2016/4/5 | No Sample | 0.612 | 0.3 | 0.012 | 0.3 | 392 | 784 | 12.25% | 4.90% | 82.76% | 18.998% | 3 | 1.836 | 18.37 | 10.00 | |
| 2016/4/5 | No Sample | 0.612 | 0.3 | 0.012 | 0.3 | 392 | 784 | 12.25% | 4.90% | 82.76% | 18.998% | 3 | 1.836 | 19.99 | 10.89 | |
| 2016/4/5 | No Sample | 0.612 | 0.3 | 0.012 | 0.3 | 392 | 784 | 12.25% | 4.90% | 82.76% | 18.998% | 3 | 1.836 | 18.77 | 10.22 | |
| 2016/4/5 | 3 Discs | 0.612 | 0.3 | 0.012 | 0.3 | 392 | 784 | 12.25% | 4.90% | 82.76% | 18.998% | 3 | 1.836 | 16.79 | 9.15 | 1.92 |
| 2016/4/5 | 3 Discs | 0.612 | 0.3 | 0.012 | 0.3 | 392 | 784 | 12.25% | 4.90% | 82.76% | 18.998% | 3 | 1.836 | 7.74 | 4.21 | 10.98 |

Table 22 shows test data of testing under inlet gas stream conditions of simulated flue gas with 20% humidity, at 150°F. When the disks were not placed in the chamber, the detected Hg° concentrations at the outlet of the chamber were 9.66 ng/L, 10.00 ng/L, 10.89 ng/L and 10.22 ng/L. After the synthetic disks were put into the chamber, Hg° concentrations were detected as: 9.15ng/L and 4.21 ng/L. The $Hg^0$ capturing capacity of the disks led to the difference of Hg° concentration in the gas stream.

| Average Hg Concentration in Flue Gas | Total Hg absorbed | Flue Temperature | Number of Discs | Disc Diameter | Calculated Average Hg Concentration on Disc | Calculated Average Hg on Disc | Efficiency |
|---|---|---|---|---|---|---|---|
| ng/L | ng | Deg. C | | cm | ng/cm^2 | ng | 100% |
| 10.19 | 42.99 | 65.0 | 3 | 2.22 | 3.70 | 14.33 | 34.46 |

Table 23: Test Result of the Mixture Gas Experiment with Moisture

The $Hg^0$ absorption efficiency and the mass of Hg° absorbed on each disk were computed as Table 23. Under the condition of simulated flue gas at 150°F with 20% humidity, the Hg° absorption efficiency of the synthetic disks was 34.46%, which was close to the Hg° absorption efficiency calculated (36.37%) under the condition of dry simulated flue gas at 150°F.

## 4.4 Discussion

Figure 29 shows a summary of the $Hg^0$ absorption efficiency results for the synthetic disks under the three flow conditions ran in these experiments, at different temperature levels.

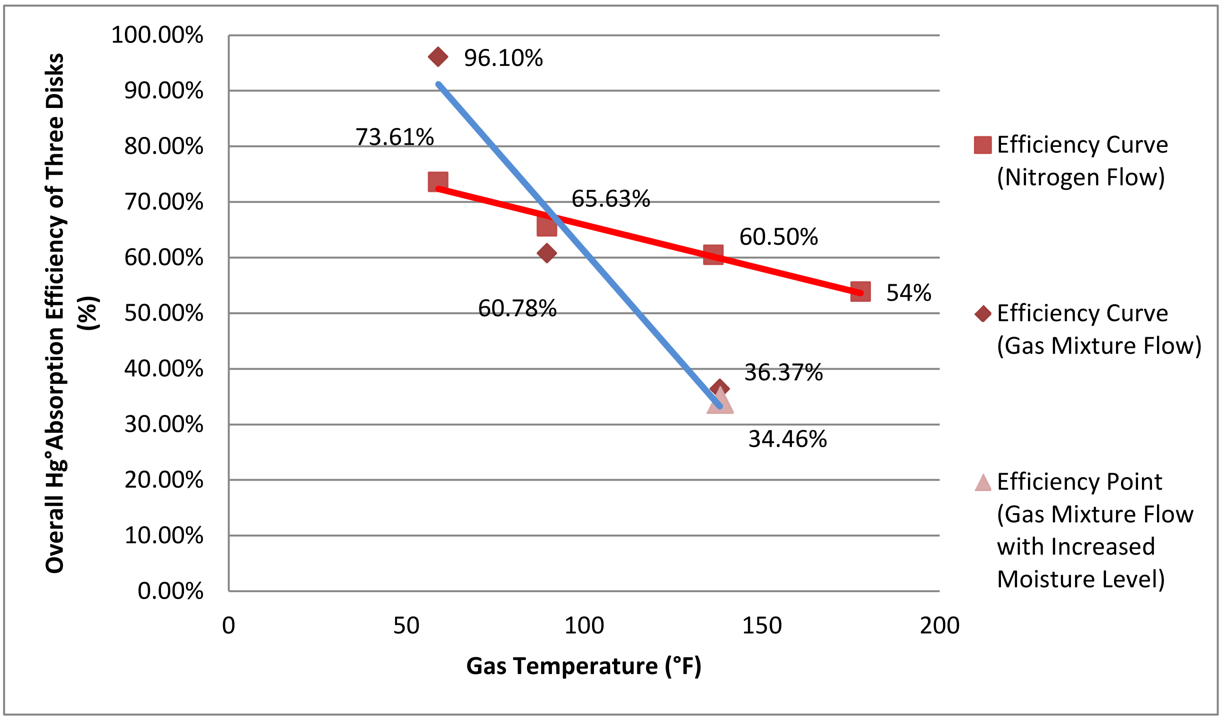


Figure 29: Summary of Hg° Absorption Efficiency Experimental Results

The plot indicates that in the simulated flue gas flow condition, there was a higher Hg° capturing efficiency of the disks at low temperature level (96.10% at 59°F) compared to that in the 100% nitrogen flow (73.61% at 59°F). However, the Hg° capturing efficiency dropped significantly with increasing gas temperature when a gas mixture was used. At a target temperature, 150°F, the Hg° absorption efficiency of the disk was 60.5% in 100% nitrogen gas, as compared to 36.37% with simulated flue gas.

For the case of a simulated flue gas mixture with increased moisture level at 150°F, the overall Hg° absorption efficiency of all three disks was 34.46%, very close to the results obtained with simulated flue gas mixture without moisture. This indicated that moisture in the gas stream has very little influence in the Hg° absorption efficiency of the synthetic disks.

# 5.0 Conclusions and Recommendations

A $Hg^0$ generation, flow and detection system was assembled to test the $Hg^0$ absorption ability of synthetic disks at different gas stream conditions. These synthetic disks would be part of a continuous $Hg^0$ monitoring system developed by UHV, Inc. and the ERC. $Hg^0$ absorption efficiency was estimated based on the a mass balance and $Hg^0$ concentration difference detected before and after placing the synthetic disks into a test chamber. It is important to achieve a good level of $Hg^0$ absorption on the disks so that the $Hg^0$ monitoring system would be able to capture significant $Hg^0$ from the flue gas for analyzer with TXRF. Modeling of the flow field inside the chamber was also performed using GAMBIT and FLUENT to estimate a more realistic value of the gas temperature at the disk positions. This helped to get an accurate relationship between the $Hg^0$ absorption efficiency and the gas temperature.

The experiments were performed under three different gas components conditions at different temperature levels. The test results indicate that the $Hg^0$ absorption efficiency of the disks is impacted respectively by the gas stream temperature. Performance of the synthetic disks is also impacted by the species typically found in activated coal-fired plant flue gas. When compared to a flow of plain nitrogen, the $Hg^0$ absorption efficiency of the disks dropped from 60.5% (at 150°F with $N_2$) to 36.37% (at 150°F with simulated flue gas). It was also found that when moisture was added to the flue gas, moisture has a very little impact on the $Hg^0$ absorption efficiency of the synthetic disks at 150°F.

The $Hg^0$ absorption efficiency of the synthetic disks varied under different gas components at different temperature levels. Further experiments would be performed in the similar flow conditions, using the TXRF system by UHV, Inc., to test the $Hg^0$ absorption efficiency of the synthetic disks. The data obtained in this study would be used to determine the accuracy of the TXRF system.

During the experiment, there are several factors that affected the accuracy of the experiments and they still could be improved:

- Because that the use of the heater in the chamber caused the burnt on the edge of the synthetic disks, the heater was not turned on. Without the heater in the chamber, it was very difficult to control the gas temperature in the chamber at temperature levels. This motivated the need to model the chamber flow field to obtain a representative value of the gas temperature in the test chamber.

- The CAVKIT is not a good steady $Hg^0$ generator, which caused the $Hg^0$ flow unsteady in some rounds of testing, affecting the experimental result, with some tests needed to be repeated a few times.

# References

[1] Liang Damei. Experimental Study of Mercury Removal with Wet Flue Gas Desulfurization System. Huazhong University of Science and Technology, Wuhan, China. 2011.

[2] Control of Mercury Emission from Coal Fired Electric Utility Boilers: An Update Air Pollution Prevention and Control Division, National Risk Management Research Laboratory, Office of Research and Development, U.S. Environmental Protection Agency, Research Triangle Park, NC. February 18, 2005.

[3] S. X. Wang, L. Zhang, G. H. Li, Y. Wu, J. M. Hao, N. Pirrone, F. Sprovieri and M. P. Ancora. Mercury Emission and Speciation of Coal-Fired Power Plants in China. Atmos. Chem. Phys. Discuss. November 12, 2009.

[4] Shaoguo Chen and Massoud Rostam-Abadi. Mercury Removal from Combustion Flue Gas by Activated Carbon Injection: Mass Transfer Effects. Electric Power Research Institute, Palo Alto, CA.

[5] Summary of Properties for Kapton Polyimide films. DuPont™.

[6] Plastic Chamber, NanoRANCH Environment Systems, LLC., Lexington, KY. 2015.

[7] Zhi Tang, Zheng Yao and Carlos Romero. Mercury Report. Energy Research Center, Lehigh University. 2015.

[8] Convective Heat Transfer Coefficient Table Chart, Engineers Edge. http://www.engineersedge.com/heat_transfer/convective_heat_transfer_coefficients__13378.html. 2016

[9] Flue gas Properties Calculator. Increase Performance Fired Process Solutions. http://www.increase-performance.com/calc-flue-gas-prop.html. 2016.

[10] PSA Sir Galahad 2 User Manual. P S Analytical. Orpington, Kent, UK.

# Vita

Hang Chen was born in the city of Huainan, China on November 11,1991. When he was four, Hang and family moved to Shanghai, China where they have remained since then. He got a Bachelor of Engineering degree in Thermal and Power Engineering after his study at Huazhong University of Science and Technology, China from 2010 to 2014. Hang began his graduate studies in Mechanical Engineering and Mechanics at Lehigh University as of the Fall 2014 semester. He is pursuing his Master of Science degree under the guidance of Dr. Alparslan Oztekin.